Structure of Magnetohydrodynamic Shock Wave

by

Chung Kung Liu

June 1967

Plasma Physics Laboratory
Report No. 67-028

Department of Space Science and Applied Physics
Catholic University of America
Washington, D.C.
20017

This research was supported by the National Aeronautics and Space Administration under Grant NGR-09-005-025.

LIST OF SYMBOLS

A	Alfven number
B	magnetic field
c	speed of light
C_p	specific heat at constant pressure
C_v	specific heat at cibstabt volume
E	electric field
e	charge of the electron
g_{ei}	$e^2/m_e m_i$ a constant
J	current density
L	scale length, Eq. (3-3)
M	Mach number
Mo	integration constant, Eq. (2-7), mass flow rate
M*	magnetohydrodynamic number, Eq. (4-16)
m_e	mass of electron
m_i	mass of ion
N	integration constant, Eq. (2-8), momentum flux
P	scalar pressure
Q	integration constant, Eq. (2-9), energy flux
Q_o	Q/u_1^2
R	gas constant
R_m	magnetic Reynold number
T	temperature

u	flow velocity
x	coordinate normal to the plane of the steady-state shock front
y	vertical coordinate in plane of steady shock wave
z	coordinate orthogonal to both x and y
β	ratio of scalar pressure to magnetic pressure
δ	percentage of charge separation
γ	ratio of specific heats
η	electric resistivity
λ_i	i^{th} characteristic value
ρ	mass density
$(\ )_1$	subscripts 1 indicate quantities at upstream
$(\ )_2$	subscripts 2 indicate quantities at downstream
$(\hat{\ })$	caps indicate dimensionless quantities
$(\ )'$	primes indicate small perturbed quantities

ABSTRACT

This dissertation studies the structure of the plane magnetohydrodynamic shock wave of a rarefied, fully-ionized plasma. Both the shock front and the magnetic field are assumed to be perpendicular to the flow direction. In the undisturbed region, the gas pressure (=nkT) can be comparable to, much smaller or much larger than the magnetic pressure ($=B^2/8\pi$), and also the magnetohydrodynamic Mach number (M*) can be any value greater than unity. Since the plasma is so rarefied that the mean-free-path here cannot be considered as a relevant scale length for the shock thickness, instead the geometrical mean of the ion and electron Larmor radius is the appropriate one. Under these assumptions, the structure of large M* shock wave is solitary wave-like, and that of the smaller M* shock waves can be either oscillatory or monotonic depending on the value of electrical resistivity.

I. INTRODUCTION

This dissertation studies the structure of magnetohydrodynamic shock waves in a rarefied, fully ionized plasma with an external magnetic field. With particular interests in that the speed of propagation of the shock front is quite high and that the gas pressure is comparable to the magnetic pressure, the former is equivalent to a high Mach number in gasdynamics and the latter implies that neither the gas pressure, i.e., the plasma temperature nor the magnetic field can be neglected. Since the plasma is very rarefied such that its ion-ion collision mean-free-path is much larger than the ion Larmor radius which, on the other hand, is much larger than the Debye shielding distance of the plasma. Moreover, the shock thickness to be found is of the order of a few geometrical mean of the ion and electron Larmor radius. Thus it can be assumed that the effect of viscosity and thermal conduction can be neglected because of the small value of the shock thickness. However, the plasma electrical resistivity, which signifies a friction between ions and electrons, is retained and behaves as the necessary dissipation mechanism in the continuum theory. For simplicity, the effect of charge separation and the self-consistent electric field are not considered in the main investigation, but as a justification they are to be computed by a perturbation method in the discussion part of this study. Application of this dissertation can be made to the bow shock formed by the interaction of the solar wind [1-5] with the magnetosphere and can also be extended to the laboratory experiments on controlled-fusion.

Previous investigations [6-14] on the structure of shock waves cannot satisfy the present model due to one or more of the following reasons: 1. no magnetic field was

considered; 2. gas pressure was neglected or only a cold plasma was considered: 3. the shock thickness considered is of the order of a few mean-free-path, which is too large to represent a shock wave here; and 4. the propagation speed of the shock front is limited to some small values.

Though it is mentioned earlier some particular interests are that the propagation speed of the shock front is quite high and that the gas pressure is comparable to the magnetic pressure, yet this analysis is so general that it covers any propagation speed of the shock front and any finite ratio of the gas pressure to the magnetic pressure.

II. BASIC EQUATIONS

With the mathematical model stated in the Introduction, the problem becomes a stationary one if the y - z plane of a cartesian coordinate system is chosen to be fixed with the shock front. Then the x-axis is the direction of flow velocity u, and the magnetic field B is specified in the z-direction. Figure 1 shows the transition region of the shock wave and the following table lists all the physical parameters:

	Upstream	Transition region	Downstream
Velocity	u_1	u	u_2
Pressure	p_1	p	p_2
Temperature	T_1	T	T_2
Density	ρ_1	ρ	ρ_2
Magnetic Field	B_1	B	B_2
Current Density	$J_1=0$	J	$J_2=0$

Here the upstream quantities are given constants. The downstream quantities are also constants but have to be determined from the classical method which was first investigated by de Hoffman and Teller [15] and later by Helfer [16]. The quantities in the transition region are functions of x and will be fully studied in this investigation.

No electric field is assumed in the stationary frame of reference, however, with the moving coordinates an apparent constant electric field $\vec{E}\left(0, \frac{u_1 B_1}{c}, 0\right)$ occurs [17,18]. It is interesting to note that $E = \frac{u_1 B_1}{c} = \frac{u_2 B_2}{c}$ is also a given constant as shown later,

although u_2 and B_2 individually are yet to be determined.

Since all physical parameters depend on the x-coordinate only, Maxwell's equation, the conservation equations for this problem, which are derived in Appendix 1, can be written here as:

$$\frac{dB}{dx} = -\frac{4\pi}{c} J \tag{2-1}$$

$$\frac{d}{dx}(\rho u) = 0 \tag{2-2}$$

$$\rho u \frac{du}{dx} = -\frac{dP}{dx} - \frac{1}{8\pi}\frac{dB^2}{dx} \tag{2-3}$$

$$\rho u \left[\frac{d}{dx}\left(\frac{u^2}{2}\right) + \frac{\gamma}{\gamma-1}\frac{d}{dx}\left(\frac{p}{\rho}\right)\right] + \frac{cE}{4\pi}\frac{dB}{dx} = 0 \tag{2-4}$$

Here the equation of state for ideal gas is used, i.e.,

$$p = \rho RT \tag{2-5}$$

In addition, the generalized Ohm's law (Appendix II) is of the form

$$\frac{dJ}{dx} + \frac{J}{u}\frac{du}{dx} + g_{ei}\frac{\rho}{u}\left[\eta J - \frac{1}{c}(cE - Bu)\right] = 0 \tag{2-6}$$

equation (2-6) gives the relation

$$E = \frac{B_1 u_1}{c} = \frac{B_2 u_2}{c}$$

which is mentioned earlier, since at both upstream and downstream regions

$$\frac{dJ}{dx} = \frac{du}{dx} = 0 \qquad \text{and} \qquad J = 0$$

Here the temperature dependence of the electrical resistivity is taken as $\eta\,(T) \propto T^{-3/2}$ which was derived by Chapman and Cowling [19] and alos by Spitzer [20].

It is further assumed that c, R, g_{ei}, and γ all are constant in this analysis.

Equations (2-2), (2-3) and (2-4) can be integrated at once, giving:

$$\begin{aligned} \rho u &= M_o = \text{constant} \\ &= \rho_1 u_1 \\ &= \rho_2 u_2 \end{aligned} \tag{2-7}$$

$$\begin{aligned} \rho u^2 + p + \frac{B^2}{8\pi} &= N = \text{constant} \\ &= \rho_1 u_1^2 + p_1 + \frac{B_1^2}{8\pi} \\ &= \rho_2 u_2^2 + p_2 + \frac{B_2^2}{8\pi} \end{aligned} \tag{2-8}$$

$$\frac{u^2}{2} + \frac{5}{2}\frac{p}{\rho} + \frac{cEB}{4\pi M_o} = Q = \text{constant}$$

$$= \frac{u_1^2}{2} + \frac{5}{2}\frac{p_1}{\rho_1} + \frac{cEB_1}{4\pi M_o} \qquad (2\text{-}9)$$

$$= \frac{u_2^2}{2} + \frac{5}{2}\frac{p_2}{\rho_2} + \frac{cEB_2}{4\pi M_o}$$

Here γ takes the value 5/3; M_o, N, and Q are integration constants and they can be evaluated by the given quantities at upstream.

Equations (2-1), (2-5) through (2-9) are the basic equations describing the coupled relations among all the physical parameters in the transition region.

III. THE GOVERNING EQUATIONS IN TRANSITION REGION AND THEIR GENERAL PROPERTIES

1. The Governing Equations in Transition Region

The four algebraic equations [(2-5), (2-7), (2-8) and (2-9)] and two differential equations [(2-1) and (2-6)] are used to describe the behavior of all the properties in the transition region. A cancellation of p, ρ, and T from the algebraic equations can be made and leaves an equation of B and u as follows:

$$u^2 - \frac{5}{4M_o}\left(N - \frac{B^2}{8\pi}\right)u - \frac{1}{2}\left(\frac{cE}{4\pi M_o}B - Q\right) = 0 \qquad (3\text{-}1)$$

further, differentiating (3-1) with respect to x and eliminating dB/dx through (2-1) gives

$$\left(Q - 2u^2 - \frac{cE}{4\pi M_o}B\right)\frac{1}{u}\frac{du}{dx} + \frac{1}{cM_o}\left(\frac{5}{2}Bu - cE\right)J = 0 \qquad (3\text{-}2)$$

Thus equations (2-6), (3-1) and (3-2) are the coupled system of only three dependent variables B, u, and J and are to be used as the governing equations in the transition region to determine the shock structure.

2. Non-Dimensional Equations

It is appropriate here to put the governing equations in a non-dimensional form by introducing the following non-dimensional variables

$$\hat{B} = \frac{B}{B_1}, \qquad \hat{u} = \frac{u}{u_1}$$

$$\hat{J} = \frac{c\eta_1}{B_1 u_1} J, \qquad \hat{x} = \frac{x}{L}$$

Here all symbols with subscript 1 denote the given physical quantities at upstream, and L is a properly chosen scale-length which is defined in equation (3-3).

Substituting these variables into equations (2-5), (3-1) and (3-2) yields

$$\hat{u}^2 - \frac{5}{4}\left(\frac{N}{M_o u_1} - \frac{B_1^2}{8\pi M_o u_1}\hat{B}^2\right)\hat{u} - \frac{1}{2}\left(\frac{B_1^2}{4\pi M_o u_1}B - \frac{Q}{u_1^2}\right) = 0$$

$$\left(\frac{Q}{u_1^2} - 2\hat{u}^2 - \frac{B_1^2}{4\pi M_o u_1}\hat{B}\right)\frac{1}{u}\frac{d\hat{u}}{d\hat{x}} + \frac{B_1^2 L}{M_o c^2 \eta_1}\left(\frac{5}{2}\hat{B}\hat{u} - 1\right)\hat{J} = 0$$

$$\frac{d\hat{J}}{d\hat{x}} + \frac{J}{u}\frac{d\hat{u}}{d\hat{x}} + g_{ei}\frac{M_o}{u_1^2}\eta_1 L\left(\frac{\eta}{\eta_1}\frac{\hat{J}}{\hat{u}^2} - \frac{1-\hat{B}\hat{u}}{\hat{u}^2}\right) = 0$$

The scale length L is defined as

$$L = \sqrt{m_e m_i}\,\frac{cu_1}{eB_1} \tag{3-3}$$

The physical meaning of L can be seen from equation (3-3) that it is the geometrical mean of the ion and electron Larmor radius. R_m and A_1 are the magnetic Reynolds number and the Alfven number defined as follows:

$$R_{m_1} = \frac{4\pi u_1 L}{c^2 \eta_1}$$

$$A_1^2 = \frac{u_1^2}{B_1^2/4\pi\rho_1}$$

Now the non-dimensional governing equations will be of the following form as:

$$\hat{u}^2 - \frac{5}{4}\left[1 + \frac{3}{5M_1^2} + \frac{1}{2A_1^2}(1 - B^2)\right]\hat{u} - \frac{1}{2}\left(\frac{\hat{B}}{A_1^2} - Q_o\right) = 0 \qquad (3\text{-}4)$$

$$\left(Q_o - 2\hat{u}^2 - \frac{\hat{B}}{A_1^2}\right)\frac{1}{\hat{u}}\frac{d\hat{u}}{d\hat{x}} + \frac{R_{m_i}}{A_1^2}\left(\frac{5}{2}\hat{B}\hat{u} - 1\right)\hat{J} = 0 \qquad (3\text{-}5)$$

$$\frac{d\hat{J}}{d\hat{x}} + \frac{\hat{J}}{\hat{u}}\frac{d\hat{u}}{d\hat{x}} + \frac{a}{\hat{u}^2}\left(\frac{\eta}{\eta_1}\hat{J} + \hat{B}\hat{u} - 1\right) = 0 \qquad (3\text{-}6)$$

Here $Q_o = \frac{Q}{u_1^2}$ and $a = g_{ei}\frac{M_o}{u_1^2}\eta_1 L$ = constant.

3. Characteristic Curves in $\hat{u} - \hat{B}$ Phase Plane

Before getting into the details of the characteristic curves it is necessary to consider the region of interest in the $\hat{u} - \hat{B}$ phase plane. Since only positive values of the flow velocity and the magnetic field are interesting in the fast-shock problem, only the first quadrant of the $\hat{u} - \hat{B}$ phase plane need be investigated (see Fig. 2). This region is further

bounded by three straight lines, (1) on the left by the minimum possible flow velocity, this is the value of flow velocity when both β_1 and M_1 go to infinity, by equation (A-3-6)

$$\hat{u}_{min} = \frac{\gamma - 1}{\gamma + 1}$$

$$= \frac{1}{4} \quad \text{for} \quad = \frac{5}{3}$$

(2) on the right by $\hat{u} = 1$, beyond which no fast shock wave can exist; and (3) bounded below by $\hat{B} = 1$, where a magnetohydrodynamic fast-shock is not possible. In the transition region, there is no upper limit for $\hat{B}$. Therefore, characteristic curves must lie above $\hat{B} = 1$ and be bounded by $\hat{u} = \frac{1}{4}$ on the left and by $\hat{u} = 1$ on the right.

There are four characteristic curves in this region that are important in this investigation, they are:

a. The locus of the downstream singularity point ($\hat{u}_2$, $\hat{B}_2$), since $B_1 u_1 = B_2 u_2$ this curve is described by the equation $\hat{B}_1 \hat{u}_1 = 1$.

b. The solution curve, in the $\hat{u} - \hat{B}$ phase plane for a given upstream Mach number and Alfven number, is described by equation (3-4).

c. The non-dimensional form of equation (2-1) is

$$\frac{d\hat{B}}{d\hat{x}} = - R_{mi} \hat{J} \tag{3-7}$$

dividing equation (3-7) by (3-5) gives

$$\frac{d\hat{B}}{d\hat{U}} = \frac{A_1^2 (Q_0 - 2\hat{U}^2 - \hat{B}/A_1^2)}{\hat{U}(\frac{5}{2}\hat{B}\hat{U} - 1)} \tag{3-8}$$

when $\frac{d\hat{B}}{d\hat{U}} = 0$, since $A_1^2 \neq 0$ and $\hat{U}$ is always finite the characteristic curve describing the locue of all maximums of the solution curve in $\hat{U} - \hat{B}$ phase plane is given by:

$$Q_0 - 2\hat{U}^2 - \frac{\hat{B}}{A_1^2} = 0 \tag{3-9}$$

d. The fourth curve is that $d\hat{B}/d\hat{U}$ can only approach infinity since the solution curve will never reach the curve $(\hat{B}\hat{U} = \frac{2}{5})$ which describes the slope going to infinity. Again it is pointed out that $\hat{U}$ is finite.

4. Definitions of Different Magnetohydrodynamic Shock Waves

As mentioned in the last section, for a given upstream Mach number M_1, the curve $\frac{d\hat{B}}{d\hat{U}} = 0$ changes its shape if the Alfven number A_1 varies. When the Alfven number is such that curves (a) and (c) (see Fig. 3) are tangent to each other, then this Alfven number is defined as the critical Alfven number and is denoted by A_1^*. Thus as $A_1 > A_1^*$, these two curves will intersect each other and this is the strong Alfven case (Fig. 4); as $A_1 < A_1^*$, these two curves do not intersect and this is the weak Alfven case (Fig. 5).

Now, different magnetohydrodynamic shock waves can be defined as follows:

a) Critical magnetohydrodynamic shock wave. This is defined as the downstream singularity point $(\hat{u}_2, \hat{B}_2)$ falling on the tangent point of curves $\hat{B}\hat{u} = 1$ and $\frac{d\hat{B}}{d\hat{u}} = 0$. Obviously this is only possible in the critical Alfven case (Fig. 3).

b) Strong magnetohydrodynamic shock waves. This is the magnetohydrodynamic shock wave that has its downstream singularity point $(\hat{u}_2, \hat{B}_2)$ on the left side of the curve $\frac{d\hat{B}}{d\hat{u}} = 0$. In other words, the solution curve started from the upstream singularity point (u_1, B_1) crossing and intersections the curve $\frac{d\hat{B}}{d\hat{u}} = 0$ to reach the point $(\hat{u}_2, \hat{B}_2)$ (Fig. 4).

c) Weak magnetohydrodynamic shock wave. When the downstream singularity point $(\hat{u}_2, \hat{B}_2)$ of a magnetohydrodynamic shock wave does not reach the curve $\frac{d\hat{B}}{d\hat{u}} = 0$, then it is defined to be a weak magnetohydrodynamic shock wave. This is only possible for the weak Alfven number case (Fig. 5).

5. General Properties in $\hat{u} - \hat{B}$ Phase Plane

There are a few general properties of this investigation which can be deduced from the characteristic curves in the $\hat{u} - \hat{B}$ plane.

a) The slope of the solution curve can be found. In the $\hat{u} - \hat{B}$ plane, as the solution curve crosses the curve $\frac{d\hat{B}}{d\hat{u}} = 0$, its slope must change sign. By equation (3-7), the slope is negative on the right-hand side of the curve $\frac{dB}{du} = 0$. The negative slope may come from two cases: (1) $\frac{d\hat{B}}{d\hat{x}} < 0$, but $\frac{du}{dx} > 0$, and (2) $\frac{d\hat{B}}{d\hat{x}} > 0$, but $\frac{d\hat{u}}{d\hat{x}} < 0$. By the arguments of the existence of a shock wave [21, 22], only the second case can be realized. Similarly, on the left-hand side of that curve, the slope is positive, since it still requires

$\frac{d\hat{u}}{d\hat{x}} < 0$ hence $\frac{d\hat{B}}{d\hat{x}}$ must also be negative. Therefore, it can be said that a weak magnetohydrodynamic shock wave always exhibits a monotonic character in $\hat{u} - \hat{B}$ phase plane, while a strong magnetohydrodynamic shock wave will overshoot to a (relative) maximum point when crossing the curve $\frac{d\hat{B}}{d\hat{u}} = 0$, afterwards, both its $\hat{u}$ and $\hat{B}$ values will decrease gradually until it reaches its downstream singularity point.

b) The curve $\frac{d\hat{B}}{d\hat{u}} \to \infty$ or $\hat{B}\,\hat{u} = 2/5$ will never influence the solution curve. This is because the locus of the downstream singularity point, or the curve $\hat{B}\,\hat{u} = 1$, will never cross this curve. By equation (3-7), this curve comes orginally from $\frac{d\hat{u}}{d\hat{x}} = 0$, thus $\frac{d\hat{u}}{d\hat{x}}$ will never be zero on the entire solution curve owing to $\hat{B}\,\hat{u} > \frac{2}{5}$.

c) Another interesting property is that the intersection point of the curve $\frac{d\hat{B}}{d\hat{u}} = 0$ and $B = 1$ changes its position due to different given upstream Mach numbers M_1 . By equation (3-7), $\frac{d\hat{B}}{d\hat{u}} = 0$ means

$$Q_o - 2\hat{u}^2 - \frac{\hat{B}}{A_1^2} = 0 \tag{3-9}$$

Evaluating Q_o by the given upstream quantities as

$$Q_o = \frac{1}{2} + \frac{3}{2}\,\frac{1}{M_1^2} + \frac{1}{A_1{}^2} \tag{3-10}$$

Substituting (3-10) into (3-9) yields

$$\frac{\hat{B} - 1}{A_1{}^2} = \frac{1}{2} + \frac{3}{2}\,\frac{1}{M_1{}^2} - 2\hat{u}^2$$

When $B = 1$, the value of $\hat{u}$ can be solved as

$$\hat{u} = \frac{1}{2}\sqrt{1 + \frac{3}{M_1^2}} \tag{3-11}$$

Equation (3-11) means that the upstream Mach number M_1 is the only factor to determine the point of intersection. In addition, M_1 must always be greater than unity in order to produce a shock wave.

6. General Properties in $\hat{u} - \hat{J}$ Phase Plane

Since characteristic curves in $\hat{u} - \hat{J}$ phase plane are very difficult to obtain, one can only catch some properties of the solution curve in this plane through its behavior in $\hat{u} - \hat{B}$ phase plane and equation (3-7), the latter relates $\hat{J}$ and $\frac{d\hat{B}}{d\hat{x}}$ directly.

For the case of weak magnetohydrodynamic shock waves, it can be seen that the solution curve in this plane must be U-shaped, i.e., the value of $\hat{J}$ decreases from the initial zero until it reaches a (relative) minimum, then increases reaching its final (zero again) value, while $\hat{u}$ decreases monotonically to its downstream value $\hat{u}_2$.

For the strong magnetohydrodynamic shock waves, one can see there is one more singular point where $\hat{J} = 0$, and $\hat{u}$ is determined by the intersection of two curves, the solution curve or equation (3-4) and the curve $\frac{d\hat{B}}{d\hat{u}} = 0$ or equation (3-9). In the neighborhood of this point, $\hat{J}$ will change rapidly from a large positive value, and equation (3-5) will be undetermined there. In the neighborhood of this point, the values of $\hat{B}$, $\hat{u}$, and $\hat{x}$ change very slowly in comparison with the changes in $\hat{J}$ thus through equations (3-5) and (3-6) one can find

the approximate expressions for J and $\frac{du}{dx}$ respectively as follows:

$$\hat{J} \cong a \frac{\hat{B}_o \hat{u}_o - 1}{\hat{u}_o^2} (\hat{x} - \hat{x}_o) \tag{3-12}$$

$$\frac{d\hat{u}}{d\hat{x}} \cong - \frac{Rm_1}{A_1^2} \hat{u}_o \left(\frac{5}{2} \hat{B}_o \hat{u}_o - 1 \right) \tag{3-13}$$

Here $\hat{B}_o$, $\hat{u}_o$ are the intersection point of equations (3-4) and (3-9), and $\hat{x}_o$ is the point $\hat{x}$ in physical space at which $\hat{B}_o$ and $\hat{u}_o$ exist.

The complete solution curve in the $\hat{u} - \hat{J}$ plane can, therefore, be obtained by equations (3-12) and (3-13).

IV. ASYMPTOTIC BEHAVIOR AT SINGULARITIES

In order to understand the behavior of the solution curves at either the upstream or the downstream singular point, it is appropriate to utilize an asymptotic analysis of the differential equations in the neighborhood of the singularities.

1. At Upstream Singularity

Since equations (3-5) and (3-6) were derived subject to a normalization by the given upstream quantities. They can be used here directly as follows:

$$\left(Q_o - 2\hat{u}^2 - \frac{\hat{B}}{A_1^2}\right)\frac{1}{u}\frac{d\hat{u}}{d\hat{x}} + \frac{R m_1}{A_1^2}\left(\frac{5}{2}\hat{B}\hat{u} - 1\right)\hat{J} = 0 \tag{4-1}$$

$$\frac{d\hat{J}}{d\hat{x}} + \frac{\hat{J}}{\hat{u}}\frac{d\hat{u}}{d\hat{x}} + \frac{a}{\hat{u}^2}\left(\frac{\eta}{\eta_1}\hat{J} + \hat{B}\hat{u} - 1\right) = 0 \tag{4-2}$$

Now, let the values of $\hat{B}$, $\hat{u}$, and $\hat{J}$ vary in the neighborhood of the upstream singularity point as:

$$\begin{aligned}\hat{B} &= 1 + B' \\ \hat{u} &= 1 + u' \\ \hat{J} &= J'\end{aligned} \tag{4-3}$$

Here primed quantities denote the small increments (decrements if they are negative) in the variables.

Substituting (4-3) into equations (4-1) and (4-2) and retaining only first order terms of increments yields:

$$(Q_o - 2 - \frac{1}{A_1^2}) \frac{du'}{dx} + \frac{3}{2} \frac{R m_1}{A_1^2} J' = 0 \qquad (4\text{-}4)$$

$$\frac{dJ'}{dx} + a (J' + B' + u') = 0 \qquad (4\text{-}5)$$

Here η/η_i, was neglected, since it is essentially unity.

Evaluating the value of Q_o by the given upstream quantities yields

$$Q_o = \frac{1}{2} + \frac{3}{2} \frac{1}{M_1^2} + \frac{1}{A_1^2}$$

Thus equation (3-9) can be written as:

$$Q_o - 2 - \frac{1}{A_1^2} = \frac{3}{2} (\frac{1}{M_1^2} - 1) \qquad (4\text{-}6)$$

Combining equations (4-4) and (4-6) gives:

$$(\frac{1}{M_1^2} - 1) \frac{du'}{dx} + \frac{Rm_1}{A_1^2} J' = 0 \qquad (4\text{-}7)$$

By the method of solving simultaneous linear differential equations, assume

$$B' = F_i e^{\lambda_i x}$$
$$u' = G_i e^{\lambda_i x}$$
$$J' = H_i e^{\lambda_i x} \qquad (4\text{-}8)$$

Substituting (4-8) into equations (4-5) and (4-7) and cancelling out the common factor yields:

$$\left(\frac{1}{M_1^2} - 1\right)\lambda_i G_i + \frac{Rm_i}{A_1^2} H_i = 0$$

$$aF_i + a G_i + (a + \lambda_i) H_i = 0 \qquad (4\text{-}9)$$

Now, by equation (3-7), F_i is related to H_i as follows:

$$F_i = - \frac{Rm_1}{\lambda_i} H_i \qquad (4\text{-}10)$$

thus, equations (4-9) can be rewritten as

$$\left(\frac{1}{M_1^2} - 1\right)\lambda_i G_i + \frac{Rm_1}{A_1^2} H_i = 0$$

$$a G_i + \left(a + \lambda_i - a \frac{Rm_1}{\lambda_i}\right) H_i = 0 \qquad (4\text{-}11)$$

The non-trivial solutions of G_i and H_i in the homogeneous equations (4-11) require that the determinant of their coefficients equal to zero, i.e.,

$$\begin{vmatrix} \left(\frac{1}{M_1^2} - 1\right)\lambda_i & \frac{Rm_1}{A_1^2} \\ a & a + \lambda_i - a \frac{Rm_1}{\lambda_i} \end{vmatrix} = 0$$

which can be expanded to

$$\left[(a+\lambda_i)\,\lambda_i - a\,Rm_1\right]\left(\frac{1}{M_1^2}-1\right) - a\,\frac{Rm_1}{A_1^2} = 0$$

or

$$\lambda_i^2 + a\,\lambda_i - a\,Rm_1\left[1+\frac{1}{A_1^2\left(\frac{1}{M_1^2}-1\right)}\right] = 0$$

Solving for λ_i gives

$$\lambda_{1,2} = -\frac{a}{2}\left\{1 \mp \sqrt{1+\frac{4\,Rm_1}{a}\left[1+\frac{1}{A_1^2\left(\frac{1}{M_1^2}-1\right)}\right]}\right\} \qquad (4\text{-}12)$$

Since the Alfven number A_1 is related to the Mach number M_1 by the equation

$$A_1^2 = \frac{\beta_1}{1.2}\,M_1^2 \qquad (4\text{-}13)$$

If we divide the values of Mach number into three regions each of which will bear a special meaning to this investigation

a) $M_1^2 > 1 + \frac{1.2}{\beta_1}$

In this region, if the terms in the square bracket under the square-root sign in (4-12) is rearranged by using (4-13), it gives

$$1 + \frac{1}{A_1^2\left(\frac{1}{M_1^2} - 1\right)} = 1 - \frac{1.2}{\beta_1 (M_1^2 - 1)} \qquad (4\text{-}14)$$

therefore, as $M_1^2 > 1 + \frac{1.2}{\beta_1}$, (4-14) is always positive. Two roots of (4-12) in this region must be of opposite signs, which signifies that the singularity point of this region is a saddle point. This turns out to be the necessary upstream condition for a magnetohydrodynamic shock.

b) $1 < M_1^2 \leq 1 + \frac{1.2}{\beta_1}$

In this region, (4-14) is always negative, then the singularity point can be of either one of the following two cases: if

$$-1 < \frac{4\,Rm_1}{a}\left[1 + \frac{1}{A_1^2\left(\frac{1}{M_1^2} - 1\right)}\right] < 0$$

λ_1 and λ_2 in (4-12) are of the same sign which signifies the singularity point in this case is a nodal-point; and if

$$\frac{4\,Rm_1}{a}\left[1 + \frac{1}{A_1^2\left(\frac{1}{M_1^2} - 1\right)}\right] < -1$$

both λ_1 and λ_2 are complex numbers. The singularity point, therefore, is a focal-point.

However, the upstream Mach number cannot be within this region, a calculation of the downstream quantities shows this case is against the thermodynamic laws [21,22].

c) $M_1^2 \leq 1$

As proved in III - 5 - (c), the upstream Mach number M_1 must always be larger than unity. Thus this region does not hold for upstream either.

In conclusion of this section, it can be said that the Mach number M_1 at upstream must fulfill the following condition:

$$M_1^2 > 1 + \frac{1.2}{\beta_1}$$

2. At Downstream Singularity

Following the same procedures as in section (1) for at upstream singularity, two roots in equation (4-12) here can be written as

$$\lambda_1 = -\frac{a}{2}\left\{1 - \sqrt{1 + \frac{4\,Rm_2}{a}\left[1 + \frac{1}{A_2^2\left(\frac{1}{M_2^2} - 1\right)}\right]}\right\}$$

$$\lambda_2 = -\frac{a}{2}\left\{1 + \sqrt{1 + \frac{4\,Rm_2}{a}\left[1 + \frac{1}{A_2^2\left(\frac{1}{M_2^2} - 1\right)}\right]}\right\} \qquad (4\text{-}15)$$

Similarly, the values of downstream Mach number M_2 *can also be divided into three* regions as follows:

a) $M_2^2 \leqslant 1$

For $M_2^2 \leqslant 1$, while Rm_2 and A_2 are always positive numbers, the values under the square-root in (4-15) are always positive and larger than unity. λ_1 and λ_2 are, therefore, of opposite signs in this region. Thus, if $M_2 \leqslant 1$, the downstream singularity point is a saddle-point.

b) $1 < M_2^2 \leqslant 1 + \frac{1.2}{\beta_2}$

In this region by the analysis in the previous section, the singularity point can be either a nodal-point or a focal-point depending on whether the value under the square-root sign in (4-15) is positive or negative. If positive, it is a nodal-point. Physically the significance of the nodal-point is monotonic shock wave behavior and that of the focal-point is oscillatory shock wave behavior. The dividing line of these zones which corresponds to the value under the square-root sign in equation (4-15) equals zero. Fig. 6 illustrates the phenomenon for the case where the Alfven number is equal to 1.2. Obviously, for other Alfven numbers similar curves can be plotted.

c) $M_2^2 > 1 + \frac{1.2}{\beta_2}$

In this region, there is only a uniform transition, therefore, no shock wave would exist.

In conclusion to the present chapter, if a magnetohydrodynamic number M^* is defined as

$$M^{*2} = \frac{M^2}{1 + \frac{1.2}{\beta}} \tag{4-16}$$

then, whenever $M^* > 1$, it signifies an upstream condition, while $M^* < 1$, a downstream condition. The latter can further be divided into a saddle-region and a nodal- of - focal-region depending on whether M_2 is larger or smaller than unity. All this information can be summarized into a plot of M^* versus β as in Fig. 7.

V. THE STRUCTURES OF MAGNETOHYDRODYNAMIC SHOCK WAVES

In chapters III and IV, the general properties of the solution curve in phase planes and its behavior in the neighborhood of the singularity points has been discussed. Now, it is the purpose of the present chapter to obtain the details of the solution curve in the physical space.

Since the coupled differential equations (3-4), (3-5) and (3-6) are highly non-linear, only a numerical method can be used to obtain the solutions. As discussed earlier in this investigation, the structures of different magnetohydrodynamic shock waves are distinct one from another, thus a study of them separately seems necessary.

1. Strong Magnetohydrodynamic Shock Waves

The characteristics of a strong magnetohydrodynamic shock wave are: (a) it is also strong Alfvenic, (b) its solution curve is not monotonic, (c) both its upstream and downstream singularity points are saddle-points, and (d) its solution curve has to cross the curve $\frac{dB}{du} = 0$.

Since both the upstream and downstream singularities are saddle-points, numerical integration must be started from the neighborhood of these two singularities. As the integrations from both sides proceed, they would meet theoretically at the intersection of equations (3-4) and (3-9). However, they can only be approached as close as possible and never be reached owing to the limit of numerical techniques. Thus, the approximate method described in III - 6 will be used to connect them in the neighborhood of this intersection point.

2. Weak Magnetohydrodynamic Shock Waves

According to the analysis given previously, the structure of weak magnetohydrodynamic shock waves are of two types, either one has a saddle-point as required for the upstream singularity, but the downstream singularities are quite different, one is a nodal-point the other a focal-point. The saddle to nodal transition exhibited a monotonic structure, and the saddle to focal gave an oscillating character. The structure for both types are computed for the same given upstream quantities except for the electrical resistivity, these and the calculated downstream quantities are as follows:

		Upstream	Downstream
Temperature	T	10^5 °K	$7.2T_1$
Magnetic field	B	24 Kilogauss	$1.5\,B_1$
Flow Velocity	u	7.36×10^7 cm/sec	$0.667\,u_1$
Pressure	p	1.38×10^5 dyne/cm^2	$10.6\,p_1$
Mach Number	M	19.85	4.92
Alfven Number	A	1.4	0.76
Magnetohydrodynamic	M*	1.4	0.75
Pressure ratio	ß	0.006	0.029
Scale length	L	3.587×10^{-3} cm	
		Monotonic case	
Electrical resistivity		10^{-13}	5.36×10^{-15}
		Oscillated case	
Electrical resistivity		10^{-14}	5.36×10^{-16}

The results of the monotonic case are tabulated in Table II and plotted in Figs. 10 and 11, and those of the oscillatory case in Table III and Figs. 12 through 14. The situation here is very similar to charging a condenser through a R-L-C circuit, where as the resistance is small it gives an oscillatory results, otherwise it is monotonic.

VI. DISCUSSION AND CONCLUSION

1. Discussion

For the model proposed in the introduction and formulated in chapter II, the structure of either strong or weak magnetohydrodynamic shocks can be obtained in the investigation. It is further found that the profile of magnetic field of a strong shock is quite different from that of a weak shock, the magnetic field in the strong shock is of the kind of a solitary wave-like while that in the weak shock is monotonically increasing to or through an oscillating transition and then reaching to the downstream value. However, the variations of other parameters, e.g., flow velocity, pressure, etc., are still in a monotonic manner as those of the weak shock.

As a justification to the assumption that the effect of charge separation is negligible, a calculation of it and the corresponding electrical field has been made by using equations (A-1-2), (A-1-6), (3-4), (3-5) and (3-6) and plotted in Figs. 15 and 16. The results are very interesting. For the strong shock wave case, in front of the singularity, the magnetic effect dominates while at the back of the fluid properties dominate thus the self-consistent field makes a sharp change there. As for the weak shock wave case, the change of the charge separation as well as the electric field is very smooth and they are small in comparison with the other terms indeed.

A further work along this investigation can be achieved by inclusion of both viscous effect and thermal conduction. These terms will not only justify the present work in the experimental controlled-fusion case where the geometrical mean of the Larmor radius of

two species is not very small in comparison with the mean-free-path, but also remove the curve $\frac{d\hat{B}}{d\hat{u}} = 0$ where a singular point present. However, one more differential equation will be added thus a whole new analysis should be involved and cannot be considered as an extension to the present investigation.

2. Conclusion

It is now appropriate to conclude this investigation by giving the following important points:

a) The structure of magnetohydrodynamic shock waves can be found for any given upstream conditions with this model. The structures, however, are different if the downstream singularity point falls in the different regimes defined in chapter IV.

b) The structure of all strong magnetohydrodynamic shock waves is similar in shape; while that of weak shocks can be of two different shapes, e.g., a monotonic and an oscillatory shape, as to determine which is the shape of a specific model, a simple calculation as derived in IV-1 can be used.

c) The magnetohydrodynamic shock wave is strong or weak depending upon both Mach number and Alfven numbers at upstream. Therefore, there is no single number which can be used to separate the strong and weak shock waves. Instead there is a curve in $\beta_1 - M_1$ plane (Fig. 17) which separates these two regions.

d) As a justification of the assumption, the mean-free-path and the geometrical mean of the electron and ion Larmor radius were calculated for the two cases considered in chapter V. The calculated values are as follows:

	Solar Wind Model	Controlled-fusion model
Mean-free-path	$4.8 \times 10^{+11}$ cm	0.31 cm
Larmor radius	2.56×10^{6} cm	3.587×10^{-3} cm

e) Unlike in the neutral gas, whose shock thickness is understood of the order of a few mean-free-paths, here it is shown that the thickness of a magnetohydrodynamic shock can be much smaller than a mean-free-path.

f) The shock thickness of the solar wind case found in this investigation is of the order of 50 km. This result agrees quite well with the observed values although a smaller electric resistivity was included in this work.

References

1. A. Bonetti, H.S. Bridge, A.J. Lazarus, E.F. Lyon, B. Rossi, and F. Scherb, Explorer X Plasma Measurements, Space Research, Vol. III, 540 (1963).

2. N.F. Ness, C.S. Scearce, and J.B. Seek, Initial Results of the IMP I Magnetic Field Experiment, J.G.R., 69, 3531 (1964).

3. C.W. Snyder and M. Neugebauer, Interplanetary Solar-Wind Measurements by Mariner II, Space Research, Vol. IV (1964).

4. Y.C. Whang and C.C. Chang, An Inviscid Model of the Solar Wind, J.G.R., 70, 4175 (1965).

5. Y.C. Whang, C.K. Liu, and C.C. Chang, A Viscous Model of the Solar Wind, Ap. J. 145, 225 (1966).

6. J.H. Adlam and J.E. Allen, The Structure of Strong Collision-Free Hydromagnetic Waves, Phil. Mag., 3, 448 (1958).

7. W. Geiger, H.J. Kaeppeler, and B. Mayser, On the Structure of Hydromagnetic Shock Waves with Transverse Field and Viscous Dissipation, Nuclear Fusion: 1962 Supplement, Part II, 403 (1962).

8. P. Germain, Shock Waves and Shock-Wave Structure in Magneto-Fluid Dynamics, Rev. Mod. Phys. 32, 967 (1960).

9. K. Hain, R. Lust and A. Schluter, Hydromagnetic Waves of Finite Amplitude in a plasma with Isotropic and Nonisotropic Pressure Perpendicular to a Magnetic Field, Rev. Mod. Phys., 32, 967 (1960).

10. M.Y. Jaffrin and R.F. Probstein, Structure of a Plasma Shock Wave, Phys. of Fluids, 7, 1658 (1964).

11. J.D. Jukes, The Structure of a Shock Wave in a Fully Ionized Gas, J. Fluid Mech., 3, 275 (1957).

12. W. Marshall, The Structure of Magnetohydrodynamic Shock Waves, Proc. Roy. Soc. London, A 233, 367 (1955).

13. R.Z. Sagdeev, The Fine Structure of a Shock-Wave Front Propagated Across a Magnetic Field in a Rarefied Plasma, Sov. Phys. - Tech. Phys., 6, 867 (1962).

14. Y.C. Whang and C.C. Chang, Structure of Weak Shock Wave in a Plasma, Phys. of Fluids. 5, 228 (1962).

15. F. de Hoffmann and E. Teller, Magneto-Hydrodynamic Shocks, Phys., Rev., 80, 692 (1950).

16. H.L. Helfer, Magneto-Hydrodynamic Shock Waves, Ap. J., 117, 177 (1953).

17. L.D. Landau and E.M. Lifshitz, The Classical Theory of Fields, Addison-Wesley Publishing Co., Reading, Mass. (1962).

18. W.K.H. Panofsky and M. Phillips, Classical Electricity and Magnetism, Addison-Wesley Publishing Co., Reading Mass. (1956).

19. S. Chapman and T.G. Cowling, The Mathematical Theory of Non-Uniform Gases, Cambridge University Press, England (1939).

20. L. Spitzer, Physics of Fully Ionized Gases, Interscience Publishers, N.Y. (1956).

21. J.E. Anderson, Magnetohydrodynamic Shock Waves, The MIT Press, Cambridge, Mass. (1963).

22. W.D. Hayes, Gasdynamic Discontinuities, Princeton University Press, N.J. (1960).

TABLE I

Numerical Solution for Strong Shock Wave

$\hat{X}$	$\hat{B}$	$\hat{u}$	$\hat{J}$	$\hat{P}$
0.1	1.002	0.99999	-0.96×10^{-4}	1.000
0.2	1.0005	0.99999	-0.2146×10^{-3}	1.000
0.3	1.0011	0.99998	-0.4799×10^{-3}	1.000
0.4	1.0025	0.99997	-0.1073×10^{-2}	1.0000
0.5	1.0056	0.99994	-0.2398×10^{-2}	1.0001
0.6	1.0125	0.99987	-0.5362×10^{-2}	1.0003
0.7	1.0279	0.99971	-0.1199×10^{-1}	1.0009
0.8	1.0624	0.99934	-0.2683×10^{-1}	1.0032
0.9	1.1296	0.99843	-0.6018×10^{-1}	1.0133
1.0	1.3137	0.99601	-0.13672	1.0609
1.1	1.7194	0.98839	-0.3278	1.3053
1.2	2.7726	0.95548	-0.9167	2.8468
1.25	3.9445	0.89535	-1.6845	6.3088
1.26	4.2819	0.87299	-1.9290	7.7223
1.27	4.6698	0.84415	-2.2282	0.6354
1.28	5.1207	0.80592	-2.6076	12.329
1.29	5.6538	0.75284	-3.1197	16.39
1.3	6.3048	0.67117	-3.9112	23.513
1.305	6.6997	0.60418	-4.5922	30.397

1.31	6.9273	0.54808	-5.2027	37.164
1.32	7.0625	0.47529	0.	47.782
1.33	6.9417	0.41924	2.9198	58.470
1.34	6.4015	0.35105	2.7694	75.843
1.35	5.9170	0.32233	2.3984	85.603
1.4	4.4688	0.2794	0.8830	105.29
1.45	3.9679	0.27147	0.2917	110.14
1.5	3.804	0.26935	0.0946	111.55
1.6	3.7338	0.2685	0.0097	112.13
1.7	3.7265	0.26842	0.0010	112.19
1.8	3.7258	0.26841	0.0001	112.20

TABLE II

Numerical Solution for Weak Shock Wave - Monotonic Case

$\hat{X} \times 10^{-2}$	$\hat{B}$	$\hat{U}$	$\hat{J} \times 10$	$\hat{P}$
0.1	1.0001	0.99994	-0.0006	1.0001
0.5	1.0002	0.99987	-0.0012	1.0002
1	1.0006	0.99969	-0.003	1.0005
1.5	1.0015	0.99924	-0.0073	1.0014
2	1.0037	0.99811	-0.0181	1.0039
2.5	1.0091	0.99534	-0.0444	1.0123
3	1.0225	0.9884	-0.1114	1.0468
3.5	1.0588	0.96893	-0.3385	1.2366
3.6	1.0733	0.96088	-0.4617	1.3506
3.7	1.0940	0.94924	-0.6803	1.5476
3.8	1.1264	0.93033	-1.1505	1.9391
3.85	1.1517	0.91519	-1.6318	2.3074
3.9	1.1891	0.89199	-2.5242	2.9490
3.95	1.25	0.85236	-4.2788	4.2082
4	1.3523	0.78094	-6.7034	6.7481
4.05	1.4651	0.69578	-4.2169	9.6906
4.1	1.5013	0.66728	-0.5158	10.523
4.15	1.5045	0.66475	-0.0284	10.591
4.2	1.5046	0.66462	-0.0012	10.594
4.3	1.5046	0.66461	-0.000	10.595

TABLE III

Numerical Solution for Weak Shock Wave - Oscillatory Case

$X \times 10^{-1}$	B	u	J x 10	P
1	1.0005	0.99975	-0.0022	1.0004
2	1.0024	0.99875	-0.0106	1.0024
3	1.0121	0.99379	-0.0525	1.0184
4	1.0627	0.96680	-0.3042	1.2649
4.2	1.0912	0.95079	-0.4920	1.5193
4.4	1.1403	0.92207	-0.8934	2.1346
4.6	1.2359	0.86175	-1.8282	3.8951
4.8	1.4313	0.72193	-3.5313	8.8395
5	1.6522	0.54454	-0.4785	11.825
5.2	1.4978	0.67006	2.6922	10.447
5.4	1.3808	0.76003	0.4114	7.5051
5.6	1.4250	0.72673	-1.4753	8.6763
5.8	1.5550	0.62409	-1.4503	11.505
6	1.5558	0.62349	1.2629	11.516
6.2	1.4612	0.69885	0.8545	9.5947
6.4	1.4507	0.70699	-0.5262	9.3343
6.6	1.5153	0.65607	-0.9451	10.815
6.8	1.5440	0.6330	0.3049	11.336
7	1.4965	0.67105	0.6734	10.420

7.2	1.4731	0.68956	-0.0876	9.8821
7.4	1.5012	0.66734	-0.5355	10.521
7.6	1.5269	0.64681	-0.0362	11.038
7.8	1.5087	0.66134	0.3952	10.681
8	1.4884	0.67745	-0.07753	10.240
8.2	1.4978	0.67004	-0.2714	10.448
8.4	1.5152	0.65619	-0.1156	10.812
8.6	1.5109	0.65959	0.1900	10.726
8.8	1.4976	0.67019	0.1082	10.444
9	1.4986	0.66942	-0.1179	10.465
9.2	1.5087	0.6614	-0.1048	10.679
9.4	1.5099	0.66058	0.0729	10.7
9.6	1.5024	0.66642	0.087	10.546
9.8	1.5005	0.66792	-0.0835	10.506
10	1.5056	0.66387	-0.073	10.614
11	1.5064	0.66322	-0.0044	10.632
12	1.5052	0.66418	0.0142	10.606
13	1.5045	0.66474	0.0071	10.592
14	1.5044	0.66476	-0.00007	10.591
15	1.5046	0.66465	-0.0016	10.594
20	1.5046	0.66462	-0.00001	10.596
25	1.5046	0.66462	0	10.596

Appendix I Derivation of Basic Equations

1. Maxwell equations

For a medium in steady-state, the Maxwell equations can be written as

$$\nabla \times \vec{B} = \frac{4\pi}{c} \vec{J}$$

$$\nabla \times \vec{E} = 0$$

$$\nabla \cdot \vec{B} = 0$$

$$\nabla \cdot \vec{E} = 4\pi e (n_e - n_i)$$

Here the permeablility is taken as unity and neglected in the equations.

For the model in this investigation, we have the following assumptions (cf. chapter I)

$$\vec{B} = \hat{k} B$$

$$E_y = \frac{u_1 B_1}{c}$$

$$\vec{J} = \hat{i} J$$

$$\nabla = \hat{i} \frac{d}{dx}$$

Here $\hat{i}$, $\hat{j}$, and $\hat{k}$ denote the unit vectors along x, y, and z direction respectively.

Therefore, the equations can be summarized as:

$$\frac{dB}{dx} = - \frac{4\pi}{c} J \qquad \text{(A-1-1)}$$

and $$\frac{dEx}{dx} = 4\pi e (n_i - n_e) \qquad \text{(A-1-2)}$$

2. Equations of conservations

The conservation equations for a system which has no viscosity, thermal conductivity and body force can be written as

$$\frac{\partial \rho}{\partial t} + \nabla \cdot (\vec{\rho} V) = 0$$

$$\rho \frac{DV}{Dt} = - \nabla p + \frac{1}{c} \vec{J} \times \vec{B} \qquad \text{(A-1-3)}$$

$$\frac{1}{2} \rho \frac{DV^2}{Dt} + \rho \frac{D}{Dt} \left(e + \frac{p}{\rho} \right) = \vec{E} \cdot \vec{J}$$

For the steady-state case with each and every parameter varying only along the x direction, we have

$$\frac{\partial}{\partial t} = 0$$

$$\frac{D}{Dt} = u \frac{d}{dx}$$

$$\nabla = \hat{i} \frac{d}{dx}$$

and that

$$e + \frac{p}{\rho} = \frac{Cv}{R} \frac{p}{\rho} + \frac{p}{\rho} = \frac{C_p}{C_p - C_v} \frac{p}{\rho} = \frac{\gamma}{\gamma - 1} \frac{p}{\rho}$$

Here $$C_p - C_v = R$$

Thus equations (A-1-2) can be written as follows

$$\frac{d}{dx}(\rho u) = 0$$

$$\rho u \frac{du}{dx} = -\frac{db}{dx} - \frac{1}{8\pi}\frac{dB^2}{dx} \qquad \text{(A-1-4)}$$

$$\rho u \frac{d}{dx}\left(\frac{u^2}{2}\right) - \frac{\gamma}{\gamma - 1}\frac{d}{dx}\left(\frac{p}{\rho}\right) + \frac{cE}{4\pi}\frac{dB}{dx} = 0$$

Equations (A-1-1) and (A-1-4) are the basic equations (2-1) through (2-4) in chapter II.

Appendix II. Derivation of the Generalized Ohm's Law

The equations of motion for each species, i.e., electron and ion, can be written as follows:

$$n_e m_e \frac{D\vec{V}_e}{Dt} = -\nabla p_e - n_e e(\vec{E} + \frac{\vec{V}_e \times \vec{B}}{c}) - n_e^2 e^2 \eta \ (\vec{V}_e - \vec{V}_i) \qquad \text{(A-2-1)}$$

$$n_i m_i \frac{D\vec{V}_i}{Dt} = -\nabla p_i + n_i e(\vec{E} + \frac{\vec{V}_2 \times \vec{B}}{c}) + n_e^2 e^2 \eta \ (\vec{V}_e - \vec{V}_i) \qquad \text{(A-2-2)}$$

Multiplying (A-2-1) and (A-2-2) by $\frac{e}{m_e}$ and $\frac{e}{m_i}$ respectively yields:

$$n_e e \frac{D\vec{V}_e}{Dt} = -\frac{e}{m_e} \nabla p_e - \frac{n_e e^2}{m_e}(\vec{E} + \frac{\vec{V}_e \times \vec{B}}{c}) - \frac{n_e^2 e^3}{m_e} \eta \ (\vec{V}_e - \vec{V}_i) \qquad \text{(A-2-3)}$$

$$n_i e \frac{D\vec{V}_i}{Dt} = -\frac{e}{m_i} \nabla p_i + \frac{n_i e^2}{m_i}(\vec{E} + \frac{\vec{V}_i \times \vec{B}}{c}) + \frac{n_e^2 e^3}{m_i} \eta \ (\vec{V}_e - \vec{V}_i) \qquad \text{(A-2-4)}$$

Subtracting (A-2-4) from (A-2-3) and neglecting terms of $\frac{m_e}{m_i}$ in comparison to unity yields

$$-\frac{D\vec{J}}{Dt} - e\vec{V}_e \frac{D n_e}{Dt} + e\vec{V}_i \frac{D n_i}{Dt}$$

$$= -\frac{e}{m_e} \nabla p_e - \frac{n_e e^2}{m_e}(\vec{E} + \frac{\vec{V}_e \times \vec{B}}{c}) - \frac{n_e e^3}{m_e} \eta \ (\vec{V}_e - \vec{V}_i) \qquad \text{(A-2-5)}$$

where

$$\vec{J} = e\,(n_i\vec{V}_i - n_e\vec{V}_e)$$

By assuming $n_e = n_i = n$, the y-component of (A-2-5) is of the form

$$\frac{dJ}{dx} + \frac{J}{u}\frac{du}{dx} + g_{ei}\frac{M_e}{u^2}\left[\eta J - \frac{1}{c}(CI - Bu)\right] = 0$$

This is basic equation (2-6).

By introducing

$$n_e = (1 + \delta)\, n$$

$$n_i = (1 - \delta)\, n$$

$$u_i = (1 + \delta)\, u$$

$$u_e = (1 - \delta)\, u$$

where $\delta = \frac{n - n_e}{n}$, $n = \frac{n_e + n_i}{2}$

The x - component of (A-2-5) can be written as follows

$$\frac{d}{dx} - \frac{n_e^2}{um_e}\eta\delta = -\frac{M_o}{4nm_eu^2}\frac{du}{dx} - \frac{B}{16\pi m_e nu^2}\frac{dB}{dx} + \frac{e}{2m_eu^2}E_x + \frac{1}{2m_ecnu^2}JB \qquad \text{(A-2-6)}$$

Appendix III. Stationary Solutions

The stationary solution (The Rankine-Hugoniot relation) of the physical properties at downstream is obtained here as a function of given physical quantities at upstream. These results not only give some insight about their variation as influenced by different given upstream conditions, but also are needed to begin obtaining solutions of the properties in the transition region.

In either upstream or downstream, the flow is uniform which signifies that

$$\frac{dJ}{dx} = 0$$

$$\frac{du}{dx} = 0$$

and

$$\frac{dB}{dx} = 0$$

The last relation further implies that

$$J = 0$$

Thus Equation (2-6) yields

$$E = \frac{B_1 u_1}{c} = \frac{B_2 u_2}{c} \qquad \text{(A-3-1)}$$

From (2-7), (2-8) and (2-9) eliminating p_2 and ρ_2 gives

$$u_2^2 - \frac{5}{4M_o}\left(N - \frac{B_2^2}{8\pi}\right) u_2 - \frac{1}{2}\left(\frac{CE}{4\pi M_o} B_2 - Q\right) = 0 \qquad \text{(A-3-2)}$$

Substituting (A-3-1) into (A-3-2) and rearranging yields

$$u_2^3 - \frac{5}{4}\frac{N}{M_o}u^2{}_2 + \frac{1}{2}Q\,u_2 + \frac{1}{8}\frac{C^2E^2}{4\pi M_o} = 0 \qquad \text{(A-3-3)}$$

Inserting M_o, N and Q by ρ_1, u_1, p_1, and B_1, there follows that $u_2 = u_1$, is a solution of (A-3-3). Factoring off $(u_2 - u_1)$, there remains a quadratic equation for u_2,

$$u_2^2 + (u_1 - \frac{5N}{4M_o})\,u_2 + (\frac{Q}{2} + u_1^2 - \frac{5N}{4\rho_1}) = 0 \qquad \text{(A-3-4)}$$

Introducing $\hat{u}_2$, the downstream to upstream velocity ratio; M_1, the upstream sonic Mach number; and β_1, the gas pressure to magnetic pressure ratio as

$$u_2 = \frac{u_2}{u_1}$$

$$M_1^2 = u_1^2 / \frac{5}{3}\frac{p_1}{\rho_1}$$

and

$$\beta_1 = p_1 / \frac{B_1^2}{8\pi}$$

Then (3-4) becomes

$$\hat{u}_2^2 - K_1 u_1 - K_2 = 0 \qquad \text{(A-3-5)}$$

Where

$$K_1 = \frac{1}{4} + \frac{3}{4M_1^2}(1 + \frac{1}{\beta_1})$$

$$K_2 = \frac{3}{20}\frac{1}{\beta_1 M_1^2}$$

The solution of u_2 that is positive is

$$\hat{u}_2 = \frac{K_1}{2} + \sqrt{\frac{K_1^2}{4} + K_2} \qquad \text{(A-3-6)}$$

Recalling that u_2 in the pure gas-dynamic shocks is

$$\hat{u}_2 = \frac{\gamma}{4} + \frac{3}{4 M_1^2}$$

Therefore, the velocity ratio of a magnetohydrodynamic shock is always greater than that of the pure gas-dynamic case, for the same given upstream Mach number.

All other physical properties at downstream can also be derived as functions of β_1 and M_1 from (2-6) through (2-9) and (A-3-6), they are

$$\hat{\rho}_2 = \frac{\rho_2}{\rho_1} = \frac{1}{\hat{u}_2} \qquad \text{(A-3-7)}$$

$$\hat{B}_2 = \frac{B_2}{B_1} = \frac{1}{\hat{u}_2} \qquad \text{(A-3-8)}$$

$$\hat{P}_2 = \frac{P_2}{P_1} = \frac{5 M_1^2}{3}(1 - \hat{u}_2) + 1 + \frac{1}{\beta_1}\left(1 - \frac{1}{\hat{u}_2^2}\right) \qquad \text{(A-3-9)}$$

$$\hat{T}_2 = \frac{T_2}{T_1} = \frac{P_2}{\hat{\rho}_2} \qquad \text{(A-3-10)}$$

$$M_2 = \frac{\hat{u}_2}{\sqrt{\hat{T}_2}} M_1 \qquad \text{(A-3-11)}$$

Equations (A-3-6) through (A-3-11) were calculated for various β_1 and M_1 values and plotted in Figures (A-3-1) through (A-3-4).

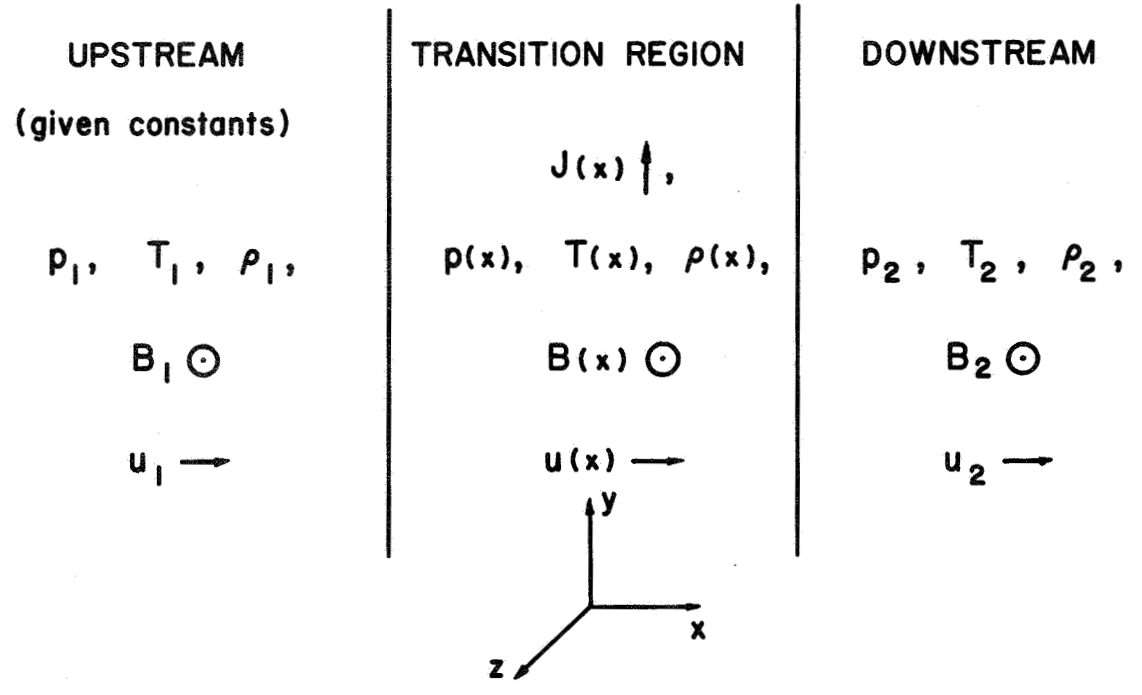

Fig. 1. A sketch of the shock wave regions.

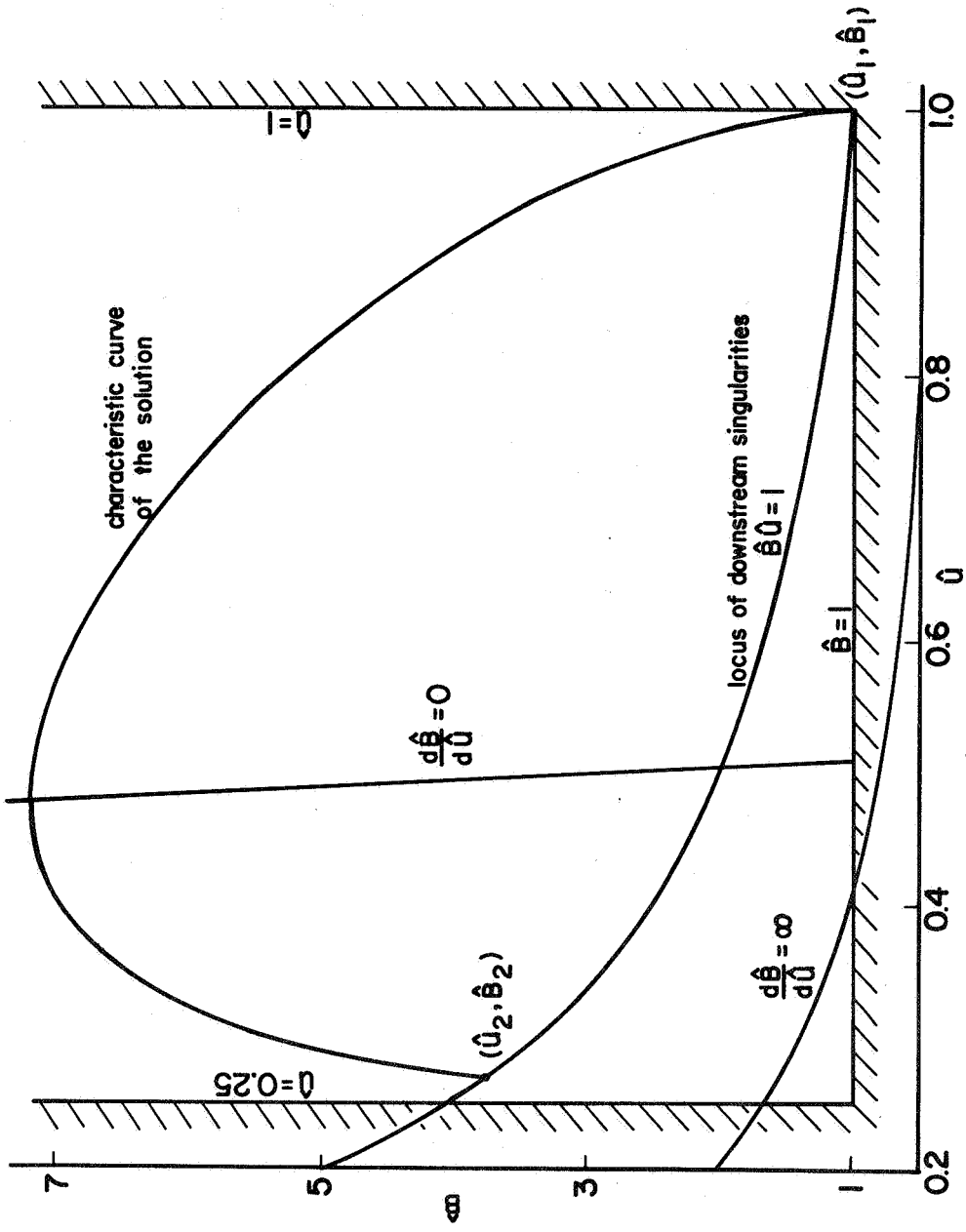

Fig. 2. Characteristic curves in $\hat{U}$-$\hat{B}$ phase plane for strong MHD shock wave for $M_1=10$, $\beta_1=1.2$.

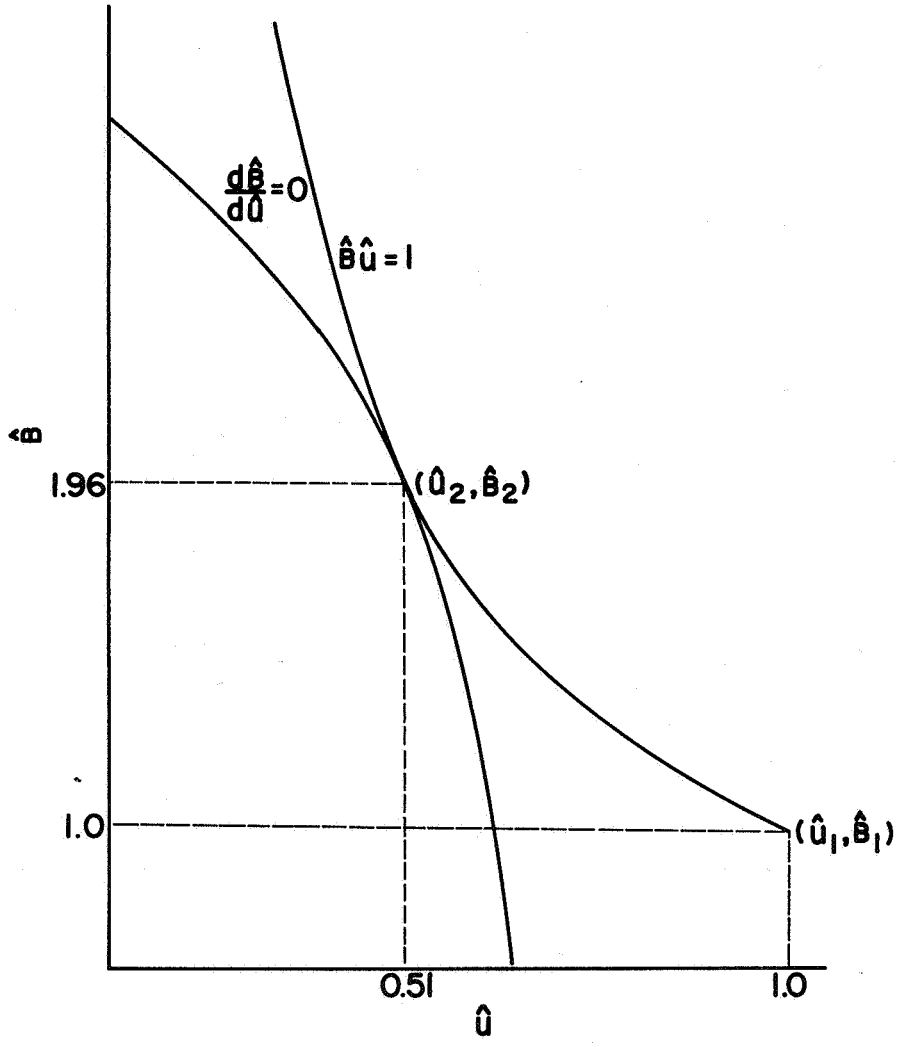

Fig. 3. Typical critical MHD shock wave case, $(\hat{u}_2,\hat{B}_2)$ is the point of tangent of the curves $\hat{B}\hat{u}=1$ and $d\hat{B}/d\hat{u}=0$.

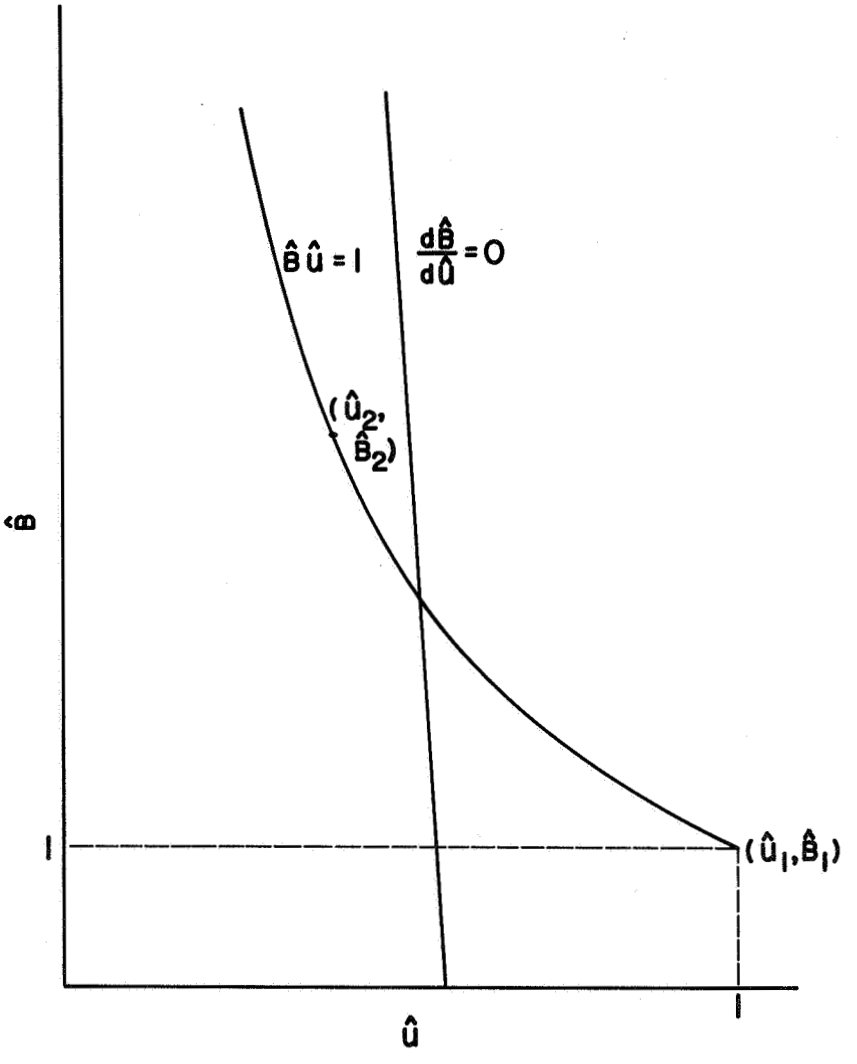

Fig. 4. Typical strong MHD shock wave case, $(\hat{u}_2, \hat{B}_2)$ is always on the left of the curve $d\hat{B}/d\hat{u} = 0$.

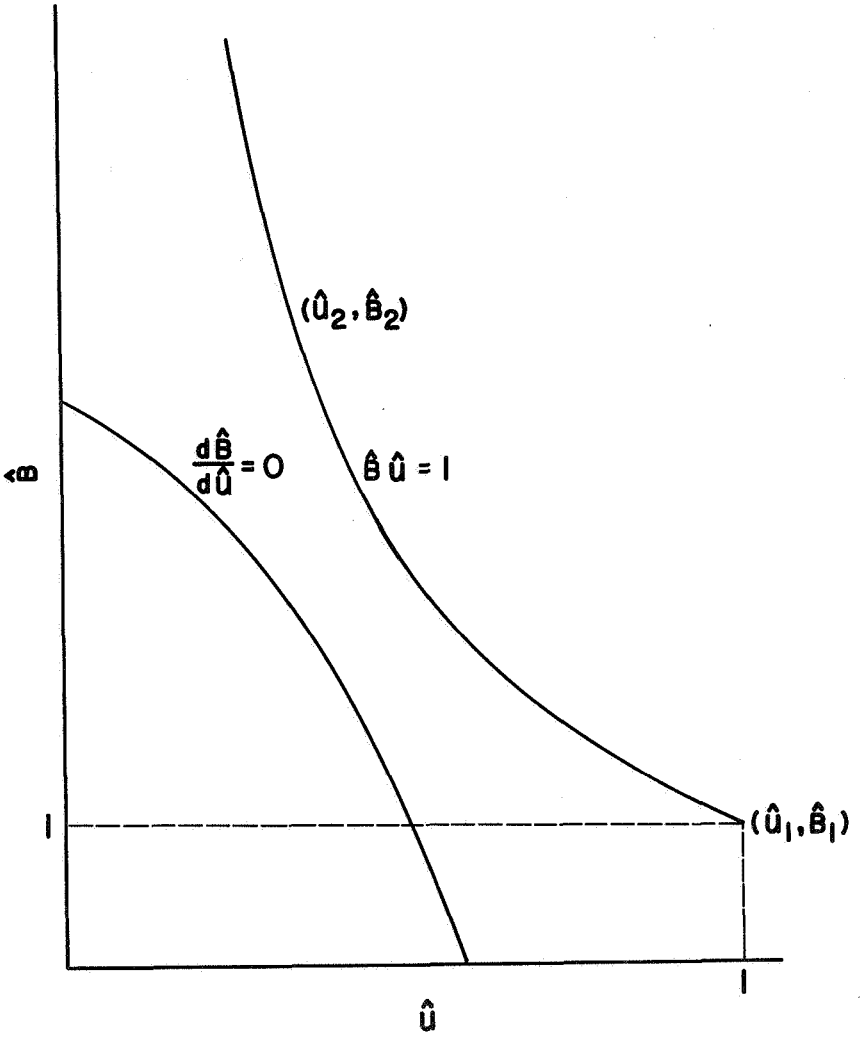

Fig. 5. Typical weak MHD shock wave case, $(\hat{u}_2, \hat{B}_2)$ is always on the right of the curve $d\hat{B}/d\hat{U} = 0$.

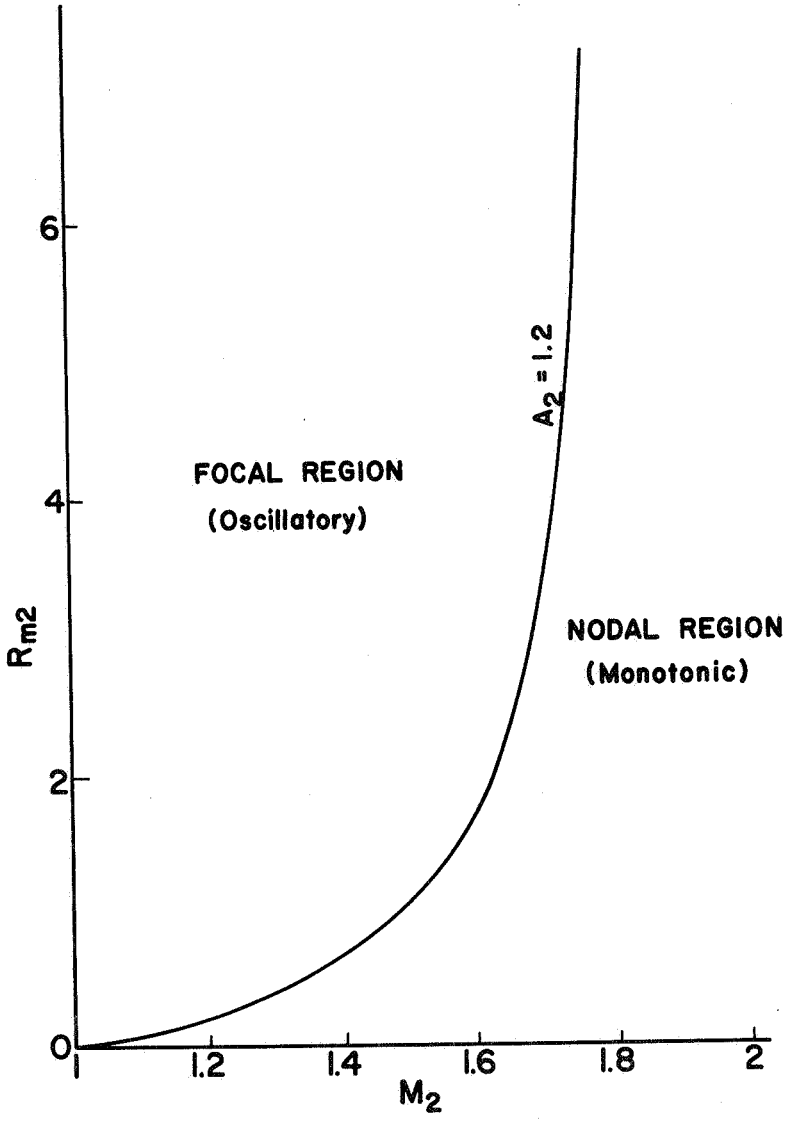

Fig. 6. Dividing line of oscillatory and monotonic regions of weak MHD shock waves for $A_2 = 1.2$.

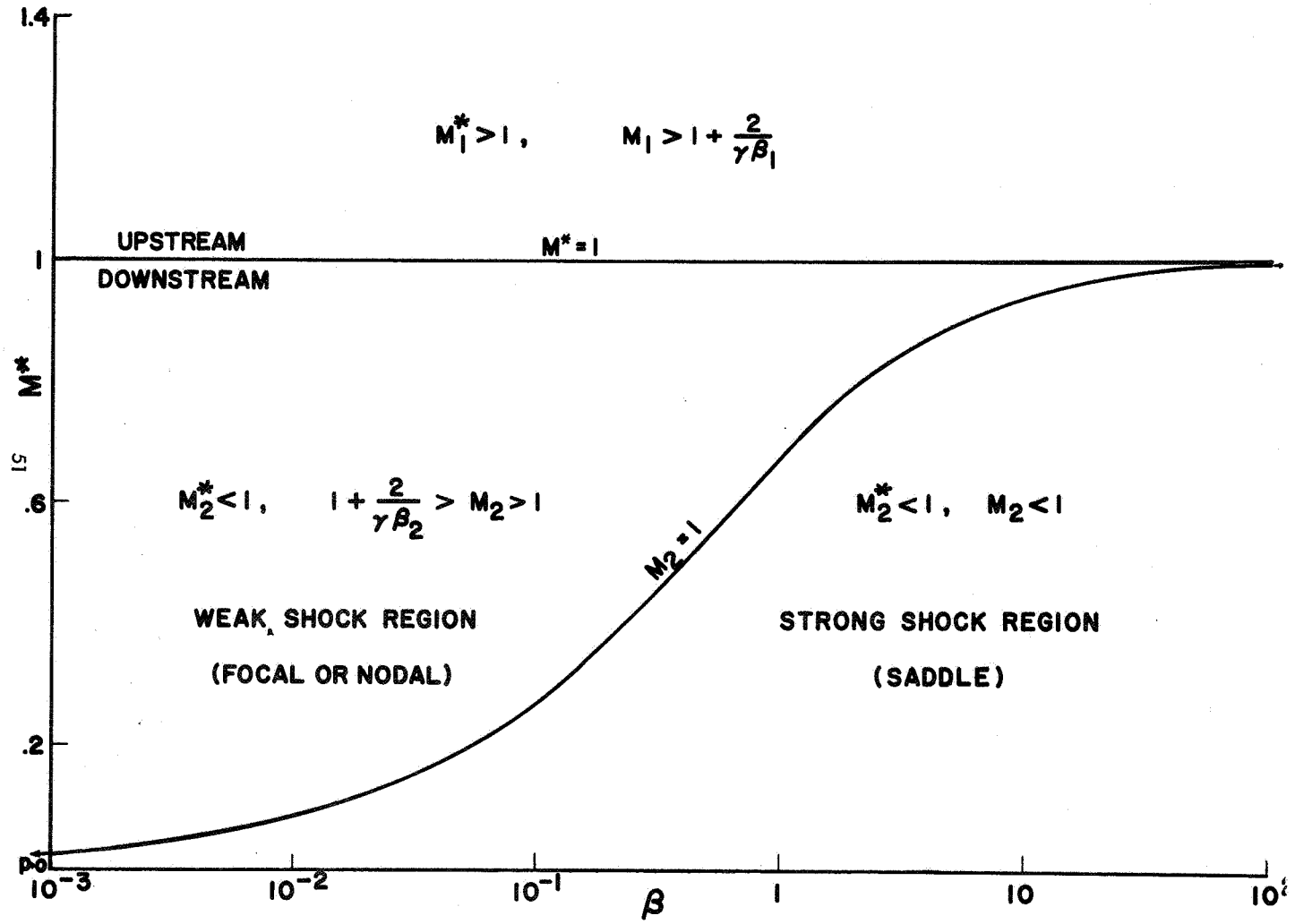

Fig. 7. Upstream and downstream regions in β - M^* plane.

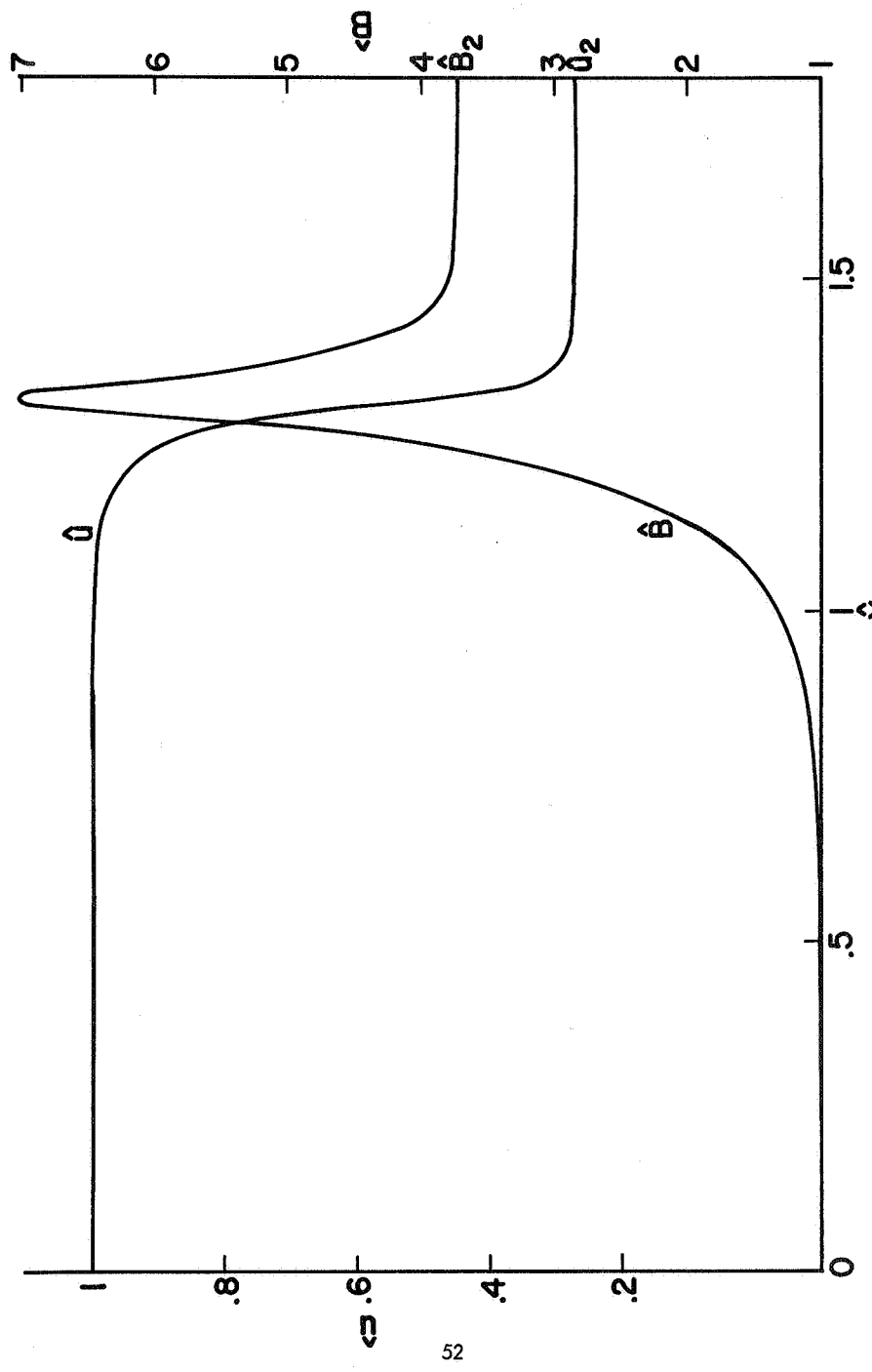

Fig. 8. Structures of $\hat{B}$ and $\hat{u}$ for strong magnetohydrodynamic shock wave.

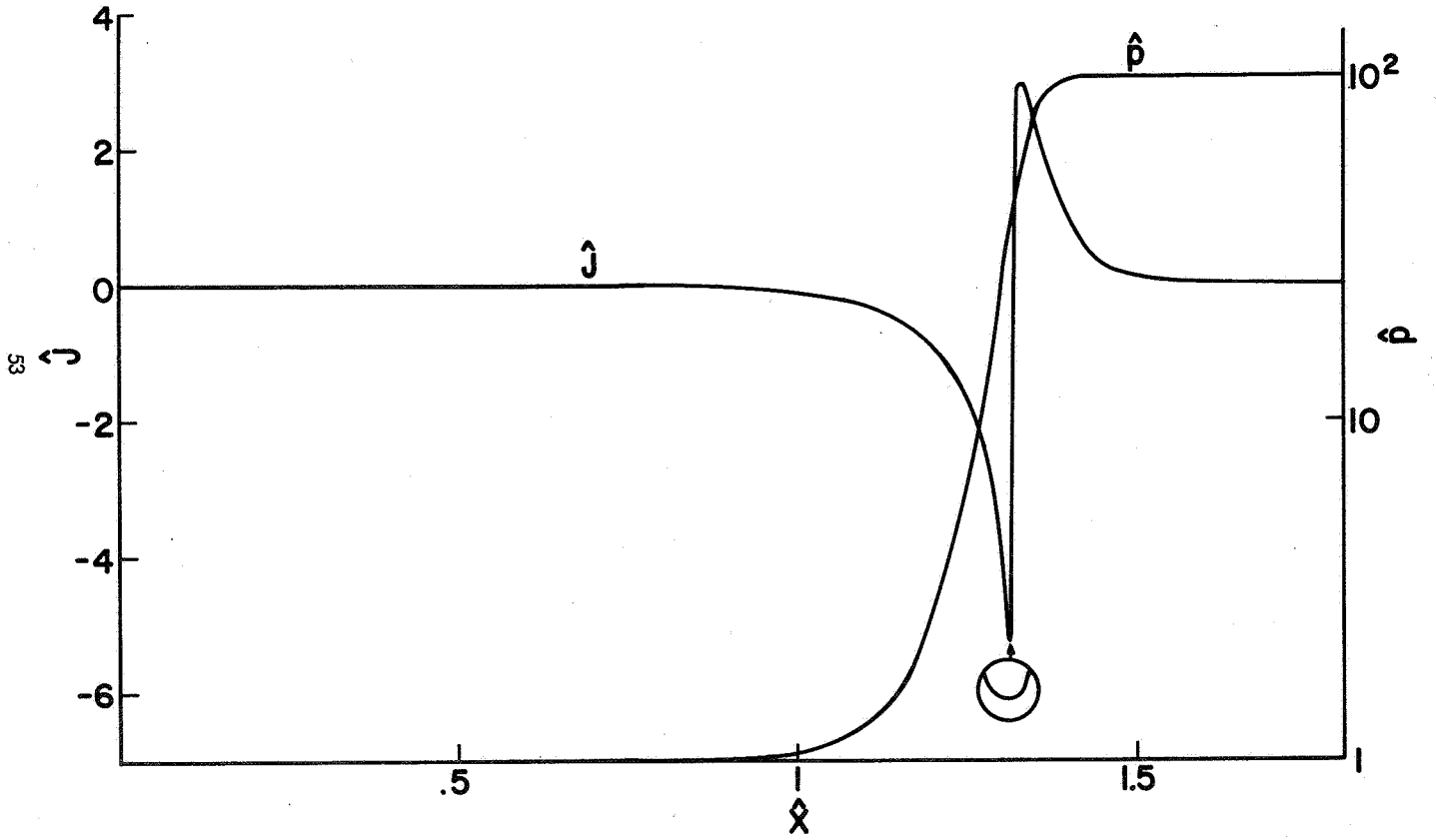

Fig. 9. Structures of $\hat{J}$ and $\hat{p}$ for strong magnetohydrodynamic shock wave.

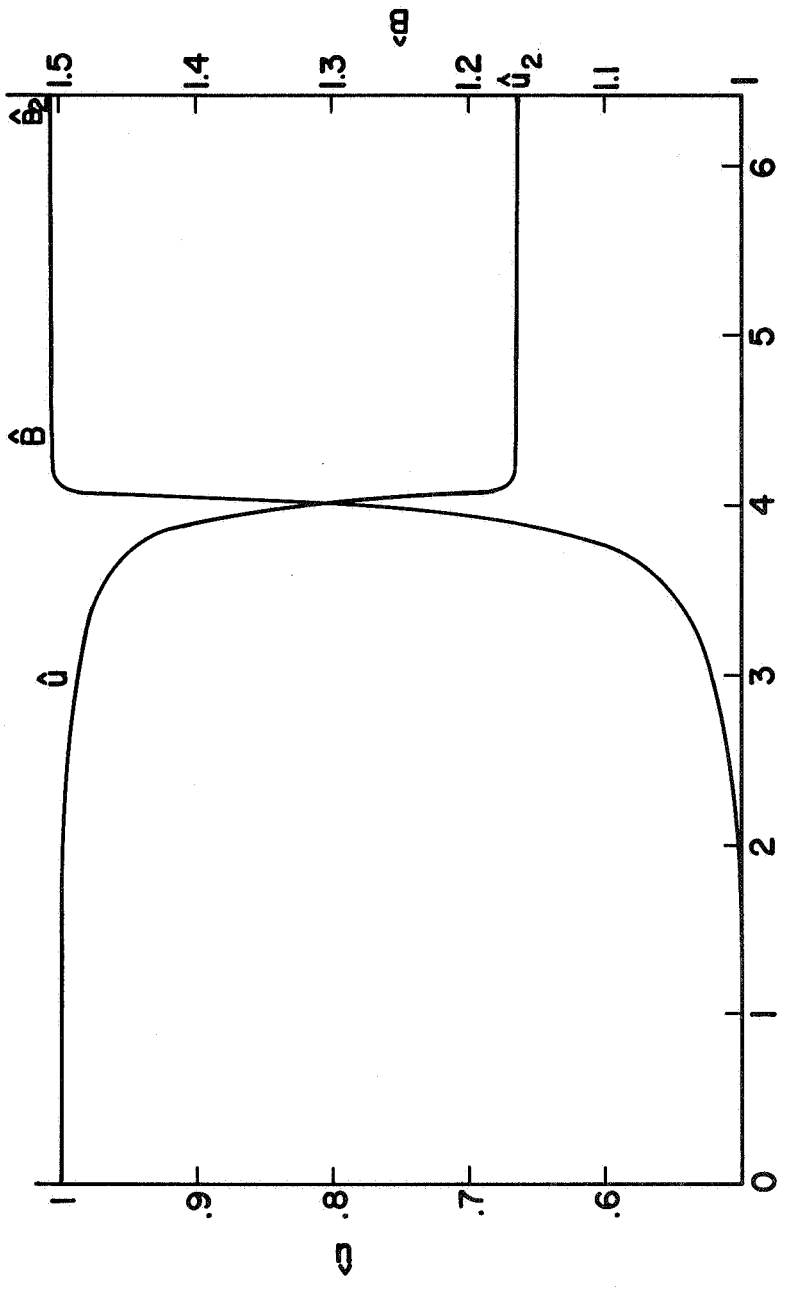

Fig. 10. Structures of $\hat{B}$ and $\hat{u}$ for weak MHD shock wave -- Monotonic case.

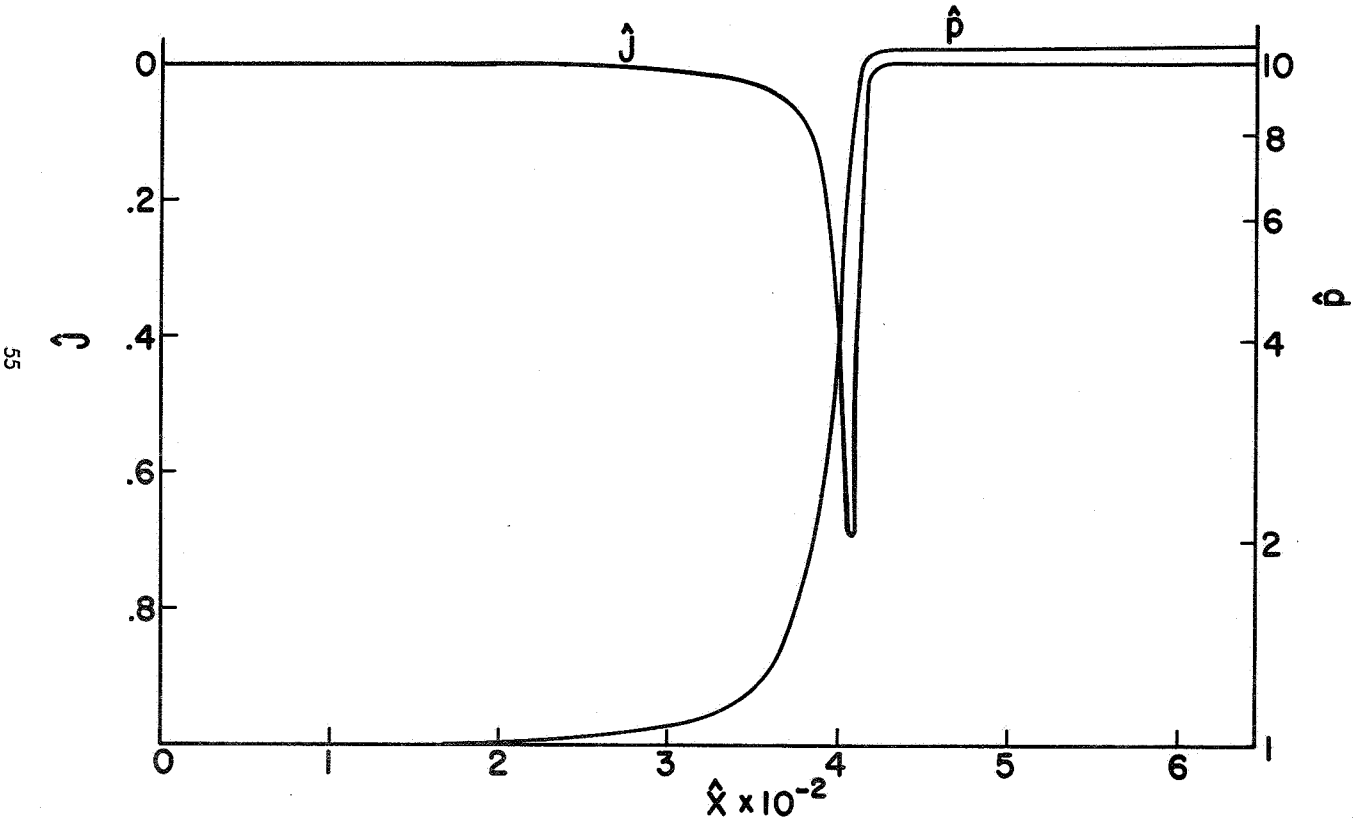

Fig. 11. Structures of $\hat{p}$ and $\hat{J}$ for weak magnetohydrodynamic shock wave - monotonic case.

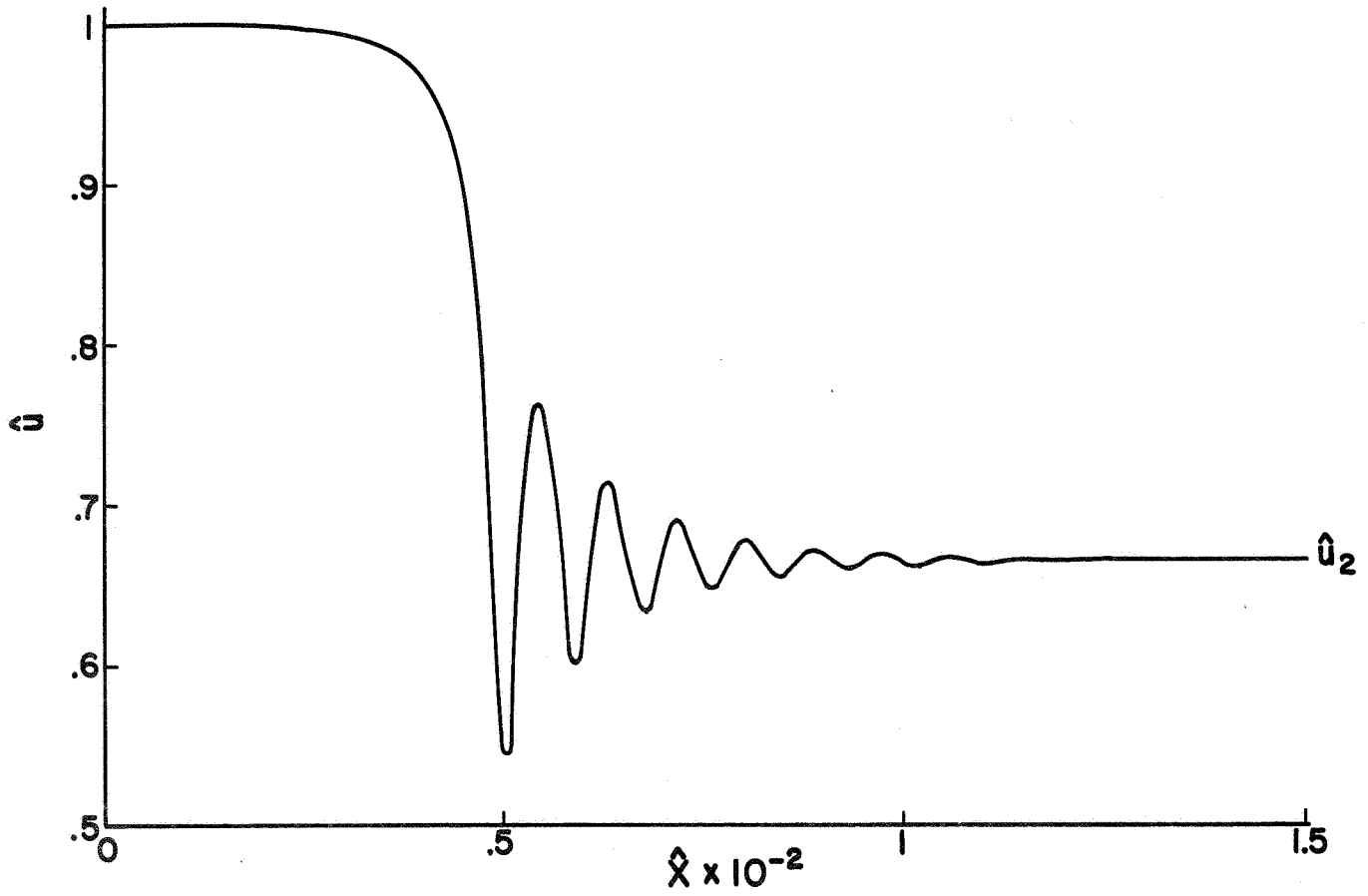

Fig. 12 Structure of $\hat{u}$ for weak magnetohydrodynamic shock wave - oscillatory case.

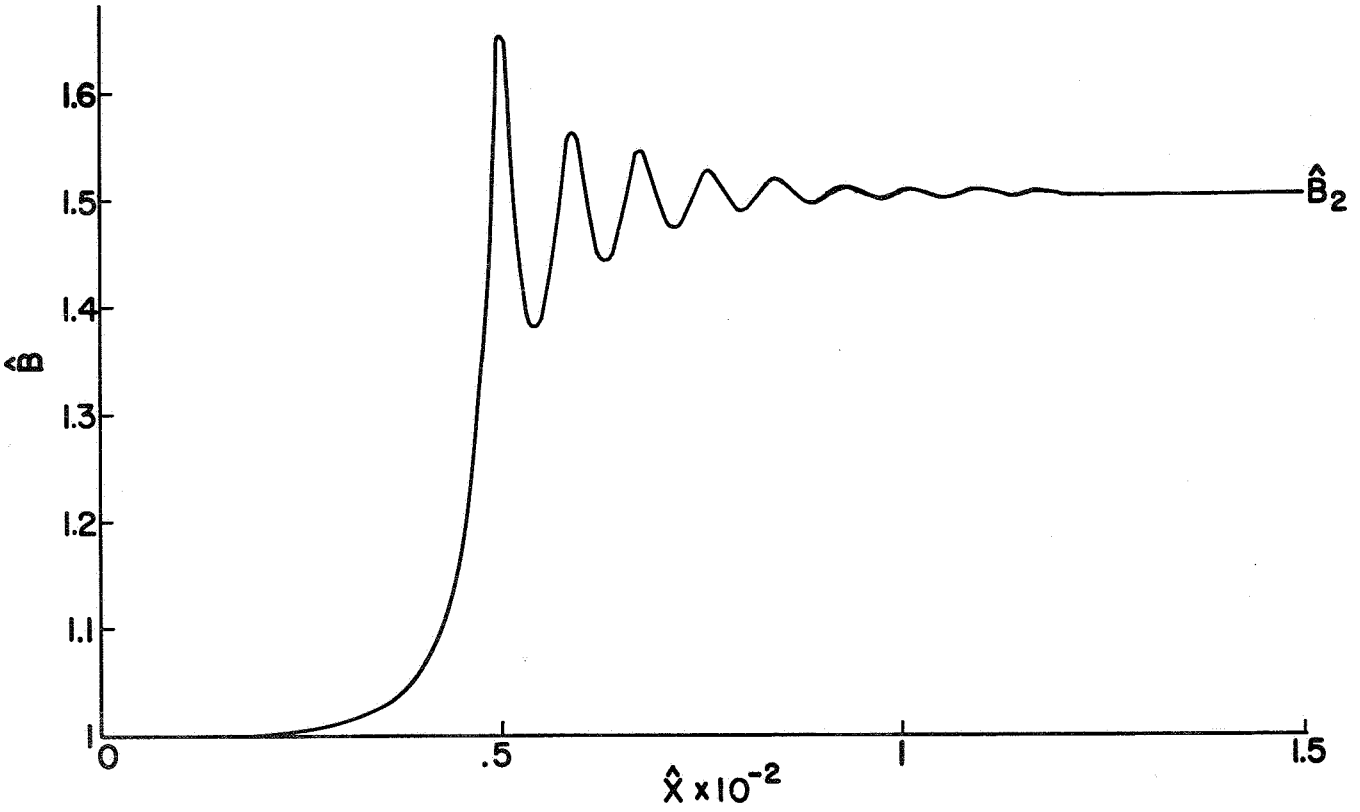

Fig. 13 Structure of $\hat{B}$ for weak magnetohydrodynamic shock wave - oscillatory case.

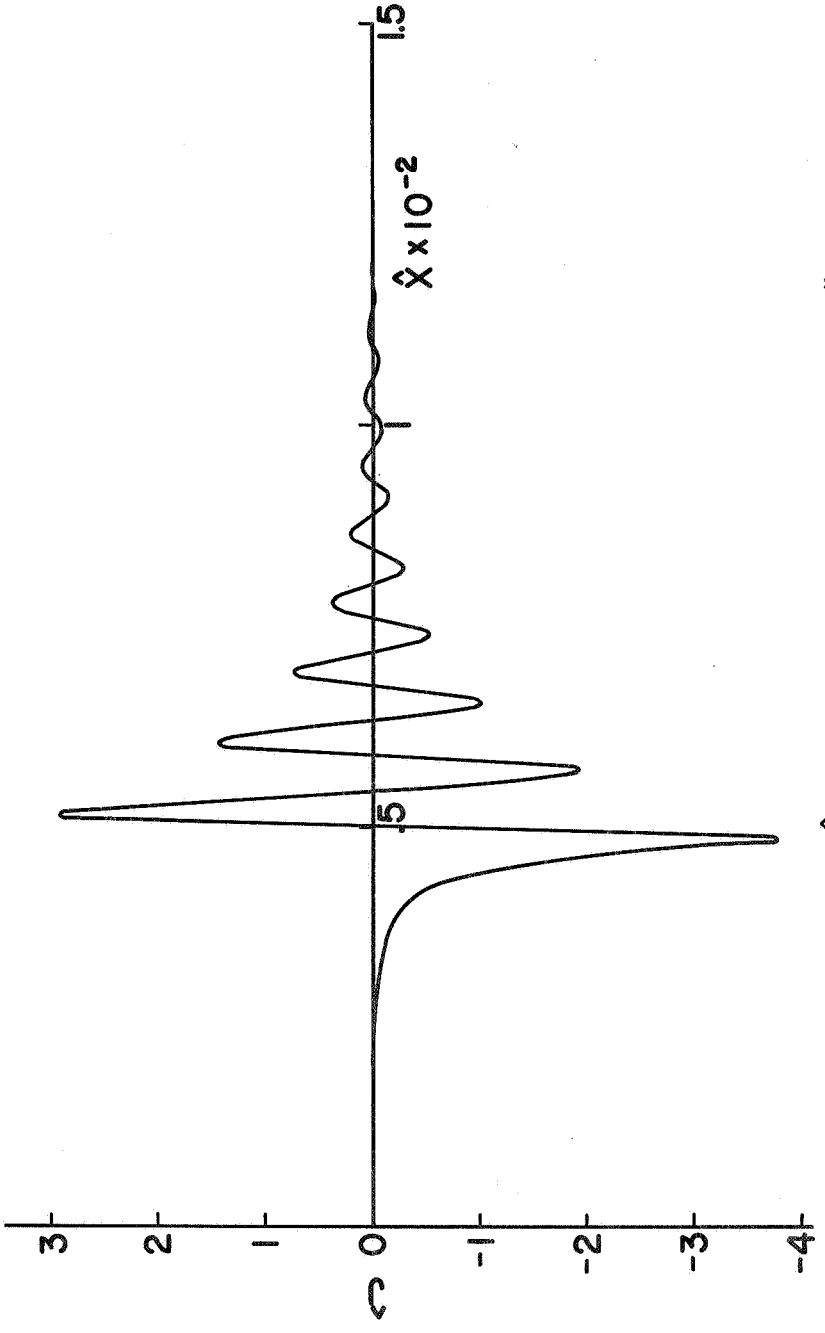

Fig. 14 Structure of $\hat{J}$ for weak magnetohydrodynamic shock wave -- oscillatory case.

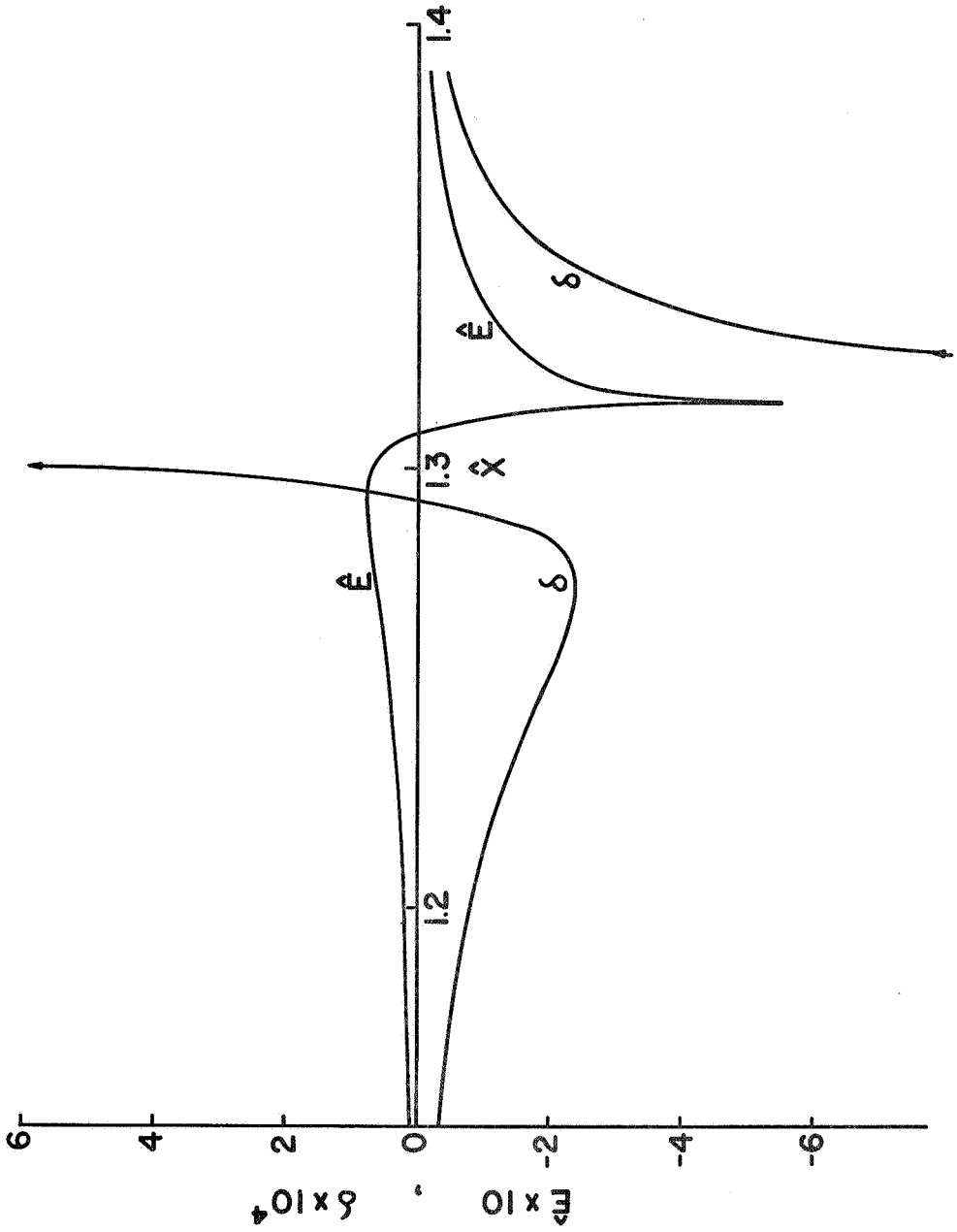

Fig. 15. Charge separation and electric field in strong magnetohydrodynamic shock wave case.

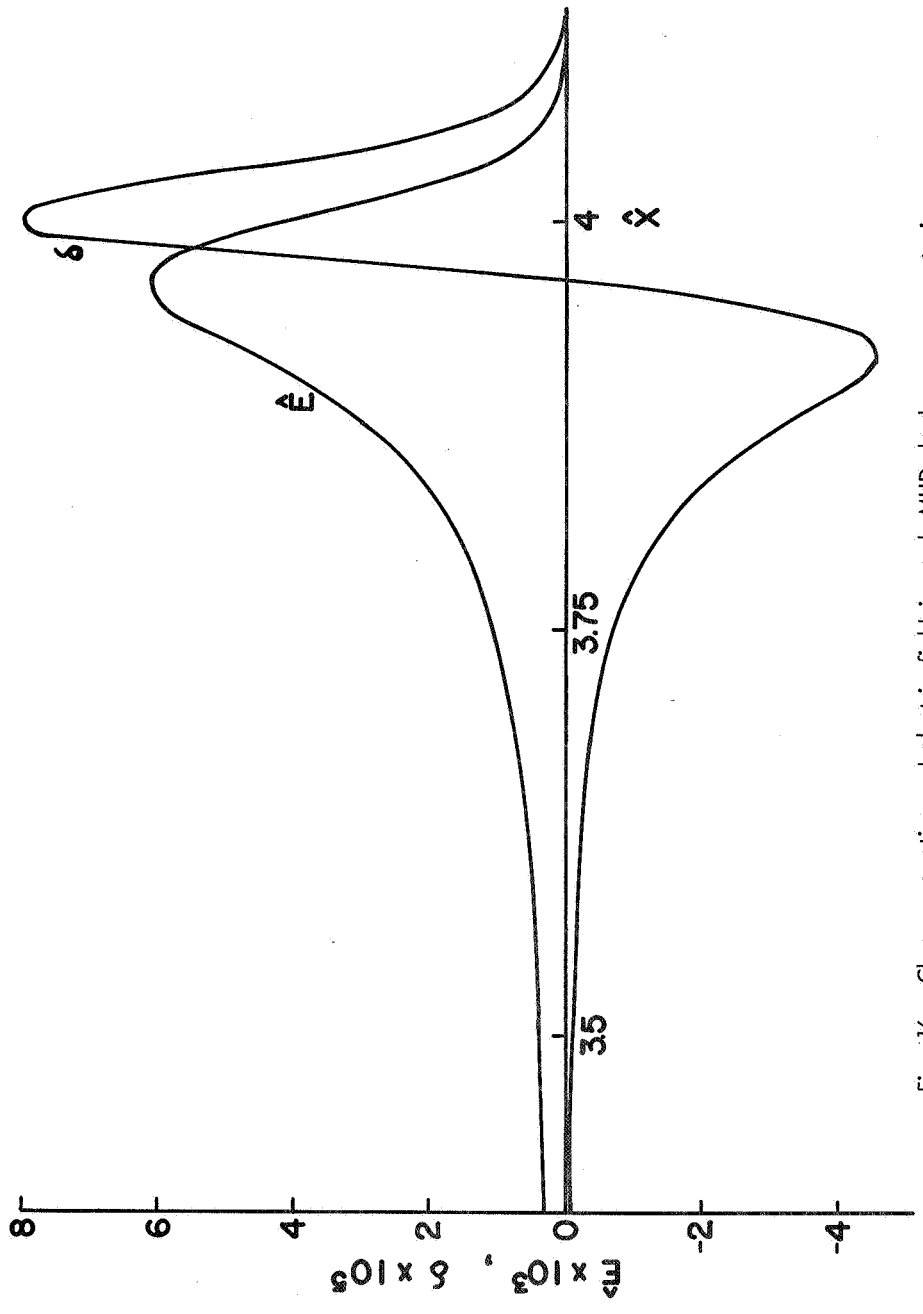

Fig. 16. Charge separation and electric field in weak MHD shock wave - monotonic case

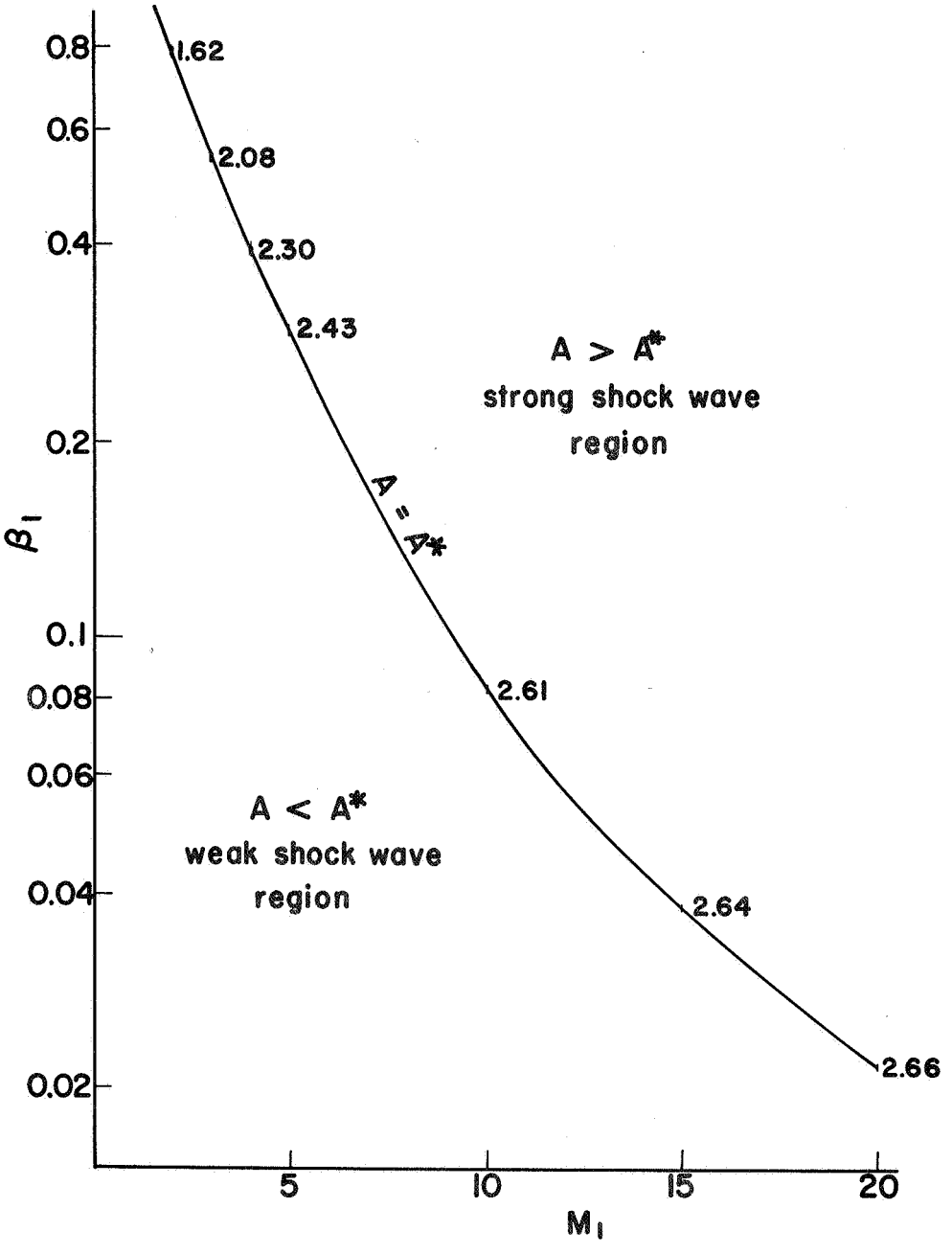

Fig. 17. Different regions of Alfvén numbers in $M_1 - \beta_1$ plane.

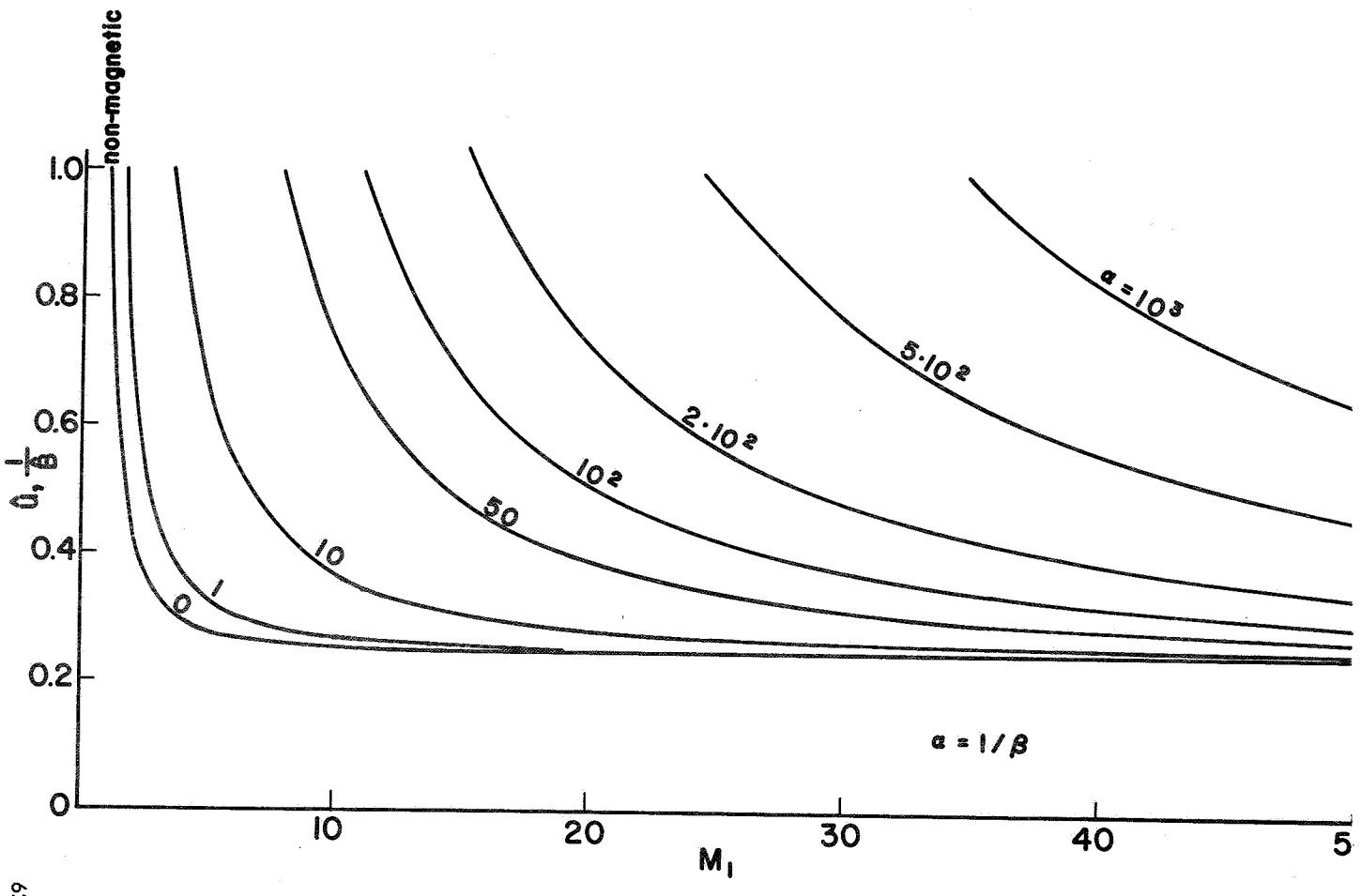

Fig. A:3.1. Downstream velocity or inverse magnetic field curves.

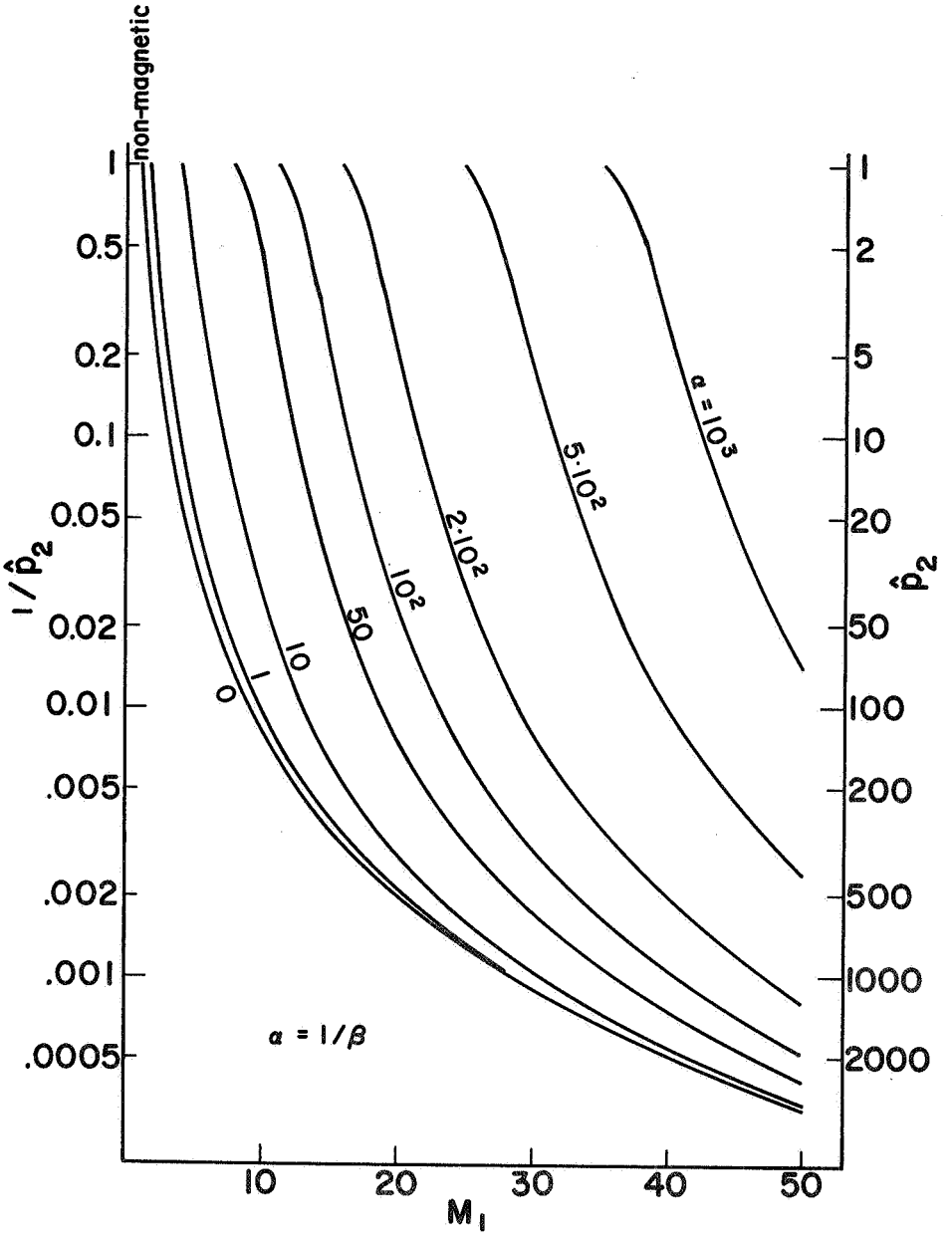

Fig. A:3.2. Downstream pressure curves.

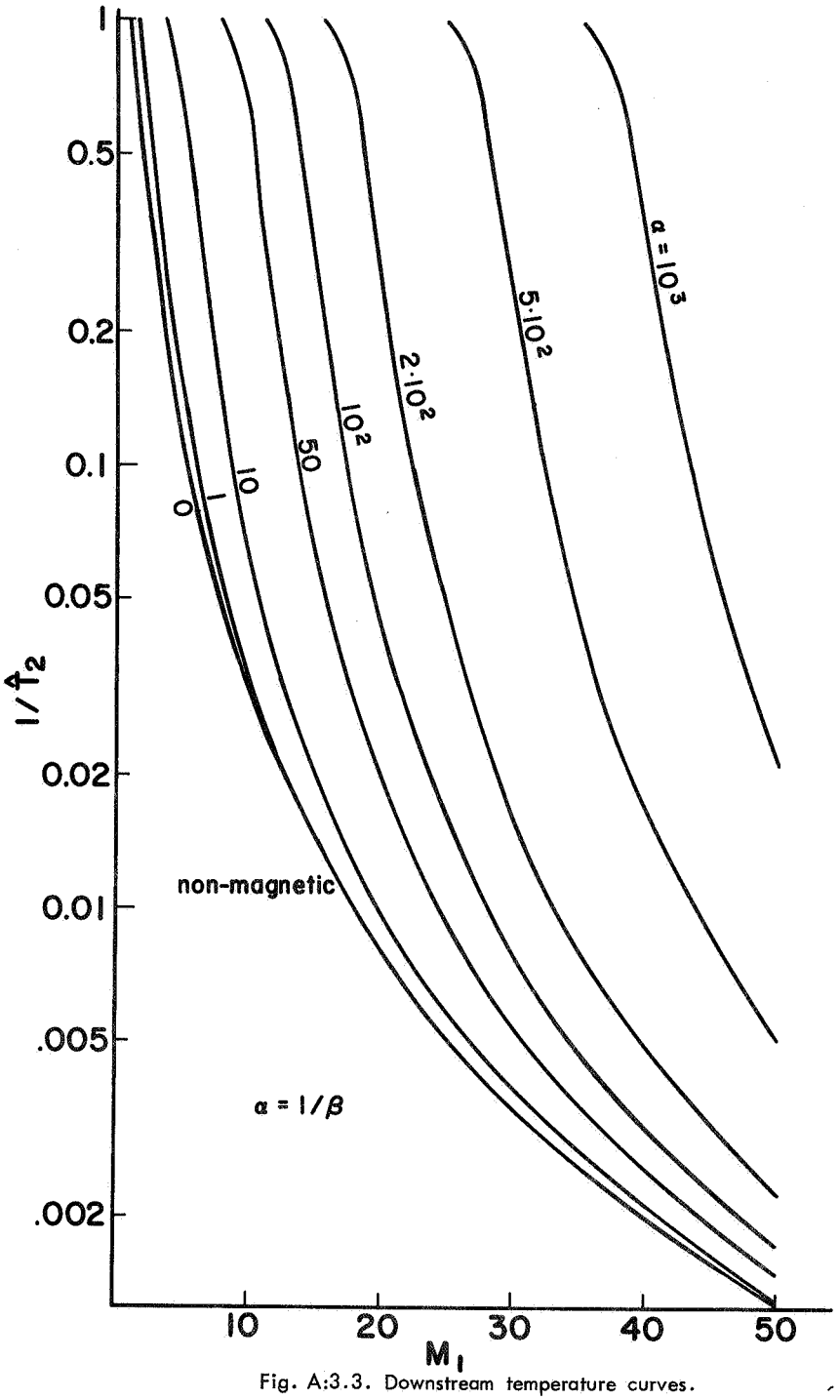

Fig. A:3.3. Downstream temperature curves.